33RD CONGRESS
OF THE INTERNATIONAL COUNCIL
OF THE AERONAUTICAL SCIENCES
STOCKHOLM, SWEDEN, 4-9 SEPTEMBER, 2022

ICAS 2022 SWEDEN

A MULTIFIDELITY MULTIDISCIPLINARY APPROACH TO UNCONVENTIONAL AIRCRAFT DEVELOPMENT AND ASSESSMENT WITH APPLICATION TO THE STRUT-BRACED-WING AND HYBRID-WING-BODY CONFIGURATIONS

David W. Zingg[1], Timothy Chau[2], Aiden L. Gray[3] & Thomas A. Reist[4]

[1]University of Toronto Distinguished Professor of Computational Aerodynamics and Sustainable Aviation; Director, Centre for Research in Sustainable Aviation.
[2]PhD Candidate, University of Toronto Institute for Aerospace Studies (Current position: Research Scientist/Engineer, Science & Technology Corporation).
[3]PhD Candidate, University of Toronto Institute for Aerospace Studies.
[4]Research Associate, University of Toronto Institute for Aerospace Studies.

Abstract

Unconventional aircraft configurations promise large improvements in energy efficiency over the current conventional tube-and-wing configuration, but their industrial adoption is impeded by significant design challenges and the associated financial and technological risks. Recent advances in optimization frameworks, including the integration of high-fidelity physical models, provide a means to address many of these challenges. However, it can be unclear how to effectively and efficiently use such models in the assessment of different unconventional aircraft configurations. The goal is to balance model accuracy and cost while also operating in a relatively large design space that facilitates the automated development of novel design features. The following questions can help formulate optimization problems that efficiently evaluate the relative performance of unconventional aircraft configurations with respect to a conventional aircraft as measured by some performance metric: 1) Which design requirements, enforced as constraints in an optimization problem, are most critical to the accurate computation of the performance metric, and which aircraft-design disciplines, *e.g.* aerodynamics, structures, weight engineering, propulsion, flight mechanics, etc., are critical in determining whether the design requirements are satisfied? 2) Which are the minimum fidelity levels needed to construct accurate and efficient physical models of the performance metric and each relevant design requirement? 3) Which design variables and constraints enable an optimizer to realize the potential of a given unconventional aircraft configuration without introducing unnecessary manufacturing difficulties or inhibiting the convergence of the optimization problem? 4) Must all design variables and relevant design requirements be considered simultaneously during optimization, or can similar conclusions be reached at a lower problem cost and complexity through a decoupled treatment? In this paper, guiding principles are proposed to answer such questions, and they are applied to formulate and solve multifidelity multidisciplinary optimization problems that efficiently and accurately evaluate the block fuel burn of two unconventional regional-class transonic airliners relative to that of a conventional tube-and-wing aircraft. The results indicate that, with current technology levels, a strut-braced-wing aircraft has the potential to burn 7.6% less fuel than an existing best-in-class conventional tube-and-wing aircraft, while a hybrid-wing-body aircraft potentially offers a 16.3% benefit. Novel and efficient design features are shown to be produced for the two unconventional configurations through optimization based on a high-fidelity aerodynamics model, thus demonstrating the importance of such models even in early investigations into unconventional aircraft.

Keywords: Optimization, Unconventional aircraft, Fuel efficiency, Strut-braced wing, Hybrid wing-body

1 Introduction

The energy efficiency of commercial aircraft must be quickly and substantially improved to mitigate their environmental impact. Various unconventional aircraft configurations have been proposed toward this end, such as the strut or truss-braced wing, the hybrid wing-body, the box wing, the double bubble, and the flying-V [1–4]. Moreover, these aircraft configurations can be combined with other future technologies to obtain reductions in energy use per passenger-kilometer beyond that provided by the configuration alone. Promising technologies include distributed propulsion, boundary-layer ingestion, and laminar flow through either active or passive means [5–7]. Further research that demonstrates how important design challenges pertaining to unconventional aircraft configurations can be addressed and credibly assesses their potential for improved energy efficiency can reduce the risk to be borne by industry in future commercialization efforts.

In the traditional approach to aircraft design, a conceptual-design phase that considers a large design space using low-fidelity analysis tools is followed by preliminary- and detailed-design phases in which the design space is reduced and the fidelity of the analysis tools is increased [8, 9]. A similar process will eventually have to be applied to any unconventional configuration that is selected for commercialization; however, it is possible to address important design challenges that may be key to achieving high energy efficiency and also to estimate the energy-efficiency benefit of an unconventional aircraft relative to, say, a conventional tube-and-wing (CTW) aircraft without carrying out a complete aircraft design. This distilled approach involves enforcing only those design requirements that have a significant effect on relative energy efficiency, which are often configuration-dependent, while operating in a relatively large design space that facilitates the automated development of novel design features. Aircraft optimization frameworks are valuable tools to perform such studies [10–16], as the relative energy efficiency of an unconventional aircraft configuration is best assessed if its design is optimized, and moreover if the reference CTW aircraft is also optimized by solving an optimization problem formulated using the same guiding principles. Given the lack of significant design experience with unconventional aircraft, it is desirable to use high-fidelity physical models during optimization to capture the complex physical phenomena that significantly contribute toward relative energy efficiency, such as those due to transonic aerodynamics. However, the reduction in computational cost obtained by only considering those design requirements and aircraft-design disciplines with a significant influence on relative energy efficiency can be further amplified by identifying the source of the sensitivity of an aircraft design to a given design requirement, as lower-fidelity physical models and fewer disciplines are often sufficient to calculate the relevant physical quantities. This is a multifidelity approach to optimization that can be used to efficiently assess the relative energy efficiency of unconventional configurations [15, 17–22]. For similar examples, see Refs. [20, 22], and for a survey of multifidelity methods, see Peherstorfer *et al.* [23].

To formulate multifidelity optimization problems that specifically aim to evaluate the relative energy efficiency of two aircraft configurations as measured by some performance metric, such as block fuel burn, judicious choices must be made with respect to several major considerations. An important question is whether to include future technologies in the problem formulation. This depends on the goal of the study, as including them reveals whether one aircraft configuration may benefit more from their adoption than another, albeit with considerable uncertainty. Conversely, excluding future technologies reveals whether an unconventional aircraft configuration may possess an inherent benefit. Since such a benefit would be realized with current technology levels, this may also lower barriers to the entry of unconventional aircraft into the market. Other major considerations are as follows: 1) Which design requirements, enforced as constraints in an optimization problem, are most critical to the accurate computation of the performance metric, and which aircraft-design disciplines, *e.g.* aerodynamics, structures, weight engineering, propulsion, flight mechanics, etc., are critical in determining whether the design requirements are satisfied? 2) Which are the minimum fidelity levels needed to construct accurate and efficient physical models of the performance metric and each relevant design requirement? 3) Which design variables and constraints enable an optimizer to realize the potential of a given unconventional aircraft configuration without introducing unnecessary manufacturing difficulties or inhibiting the convergence of the optimization problem? 4) Must all design

variables and relevant design requirements be considered simultaneously during optimization, or can similar conclusions be reached at a lower problem cost and complexity through a decoupled treatment? Specialized computational tools are needed to solve the resulting multifidelity multidisciplinary optimization problems, as they often require combining a large design space comprising both local and global geometric design variables with high-fidelity analyses, at least for aerodynamics [17, 21]. This leads to the requirement of aerodynamic shape optimization frameworks [10–12, 24] and sometimes aerostructural [25, 26] or aeropropulsive optimization frameworks [27, 28] capable of handling a large number of design variables and being robust to large geometric changes. The latter requirement necessitates the development of robust strategies for geometry control and grid deformation [10, 29].

The objective of this paper is to propose and apply guiding principles that can be used to answer the four questions posed above. The answers vary depending on the aircraft configuration considered, but they lead to the formulation of multifidelity multidisciplinary optimization problems in all cases. The following topics are covered: the choice of a suitable performance metric by which to compare aircraft configurations, the choices of a suitable reference aircraft, corresponding nominal and sizing missions, and technology levels, and the choices relevant to the four questions posed above, which are centered on the critical design requirements and disciplines and their implications on physical-model fidelity levels, the design variables and constraints, and the optimization problem structure. The paper also presents a specialized multifidelity multidisciplinary optimization framework used to solve the formulated optimization problems and two comparative studies: assessments of regional-class strut-braced-wing (SBW) and hybrid-wing-body (HWB) aircraft, both in relation to an existing best-in-class CTW aircraft. The HWB aircraft is optimized with and without assuming full reliance on variable-length landing gear to achieve rotation for takeoff, leading to a discussion on a method of verifying whether select design requirements indeed have a significant effect on the performance metric.

2 An Approach to the Assessment of Aircraft Configurations

The approach proposed in this paper to assess the potential of unconventional configurations has three stages: 1) the selection of a performance metric with respect to which different aircraft configurations can be compared and optimized, 2) the selection of a reference aircraft, a nominal mission, one or more sizing missions, and target technology levels, and 3) the formulation of multifidelity multidisciplinary optimization problems that take into account the performance metric and the nature of the aircraft configurations under consideration.

2.1 Selection of a Metric for Aircraft Performance Comparisons

The performance metric is a high-level quantity, or a combination thereof, that can be credibly computed and therefore used to compare different aircraft configurations. A performance metric that is relevant to both the economic and environmental interests of industry is block fuel burn, as an aircraft that burns a minimum amount of fuel has low operating costs and greenhouse-gas emissions [21]. Alternatively, maximum takeoff weight (MTOW) [17, 19] and direct operating costs [30] are two other often-used metrics that place additional emphasis on the economic interests of industry by providing relatively low airport landing fees and manufacturing costs. Climate-change impact can also be used as a performance metric, albeit with relatively large modeling uncertainties [31, 32]; if future technologies are considered, minimizing climate-change impact requires some speculation about future combustor technologies and fuels in terms of their potential to reduce nitrogen oxide emissions.

It may be useful to optimize some weighted average of performance-metric values taken over multiple cruise operating conditions that are likely to be encountered in airline service. This method, known as multipoint optimization, improves (or at least ascertains) robustness to variability mainly in the cruise Mach number and lift coefficient, and it reduces the likelihood that a design is point-optimized and thus performs relatively poorly in slightly off-design cruise conditions while performing exceptionally well at the design point [33–36]. In addition, a combination of performance metrics can be simultaneously optimized, giving rise to a Pareto front that can be used to examine the trade-offs due to their

competing nature [37, 38].

2.2 Selection of a Reference Aircraft, Nominal and Sizing Missions, and Technology Levels

One of the goals of a comparative aircraft study is to credibly quantify any benefit that one configuration may possess over another. When comparing unconventional configurations to a CTW configuration, the latter could be either 1) an existing best-in-class CTW aircraft, 2) a CTW aircraft optimized with significant design freedom and current technology levels, or 3) a CTW optimized with significant design freedom and future technologies that could conceivably be available when the unconventional aircraft considered is forecast to enter the market. Whether to consider future technologies such as flow control, boundary-layer-ingesting engines, and distributed propulsion depends on the goal of the study. If the goal is to determine whether an unconventional configuration alone is sufficient to confer a significant performance benefit, then Option 1 or 2 should be chosen. Option 3 has high uncertainty, as many physical models of future technologies are not yet mature, but it implies that each aircraft will be optimized to take full advantage of the future technologies, which may disproportionately benefit one configuration. Thus, if the goals of a study include determining the benefit conferred by synergistic effects, then Option 3 should be chosen. Nonetheless, omitting future technologies will reveal to what degree an unconventional aircraft may be expected to outperform a CTW aircraft even with current technology levels, thus potentially lowering the barriers to its entry into the market. Option 2 can be chosen to study the possible benefits of design freedom that was precluded in existing CTW aircraft for various reasons. For example, wing span and sweep could be freed consistently with Option 2 in conjunction with cruise altitude and Mach number in case performance can thus be improved irrespective of the restrictions on altitude and Mach number implicit in Option 1. For the reasons discussed above, Option 1 may provide the least uncertain comparison, Option 2 may provide the fairest comparison, and Option 3 may provide the most complete comparison, which is also the most optimistic if an unconventional aircraft benefits more from future technologies than a CTW aircraft.

To further ensure a fair comparison, the following *mission variables* can be made equal across each compared aircraft configuration: the range, the payload, the cruise Mach number, and the notional mission profile. This applies to the nominal mission and also to a number of critical sizing missions. The nominal mission is the most commonly flown, and that for which the performance metric is calculated, while the sizing missions are representative of the intended maximum capabilities of the aircraft in terms of payload and range; they are often flown starting from MTOW. Allowing variable initial cruise altitudes is particularly important for unconventional configurations, as many are inherently more efficient at relatively high cruise altitudes that are not easily foreseen without recourse to optimization [4]. Although engine performance implicitly limits altitude, an explicit upper bound on altitude can also be enforced because of increasingly high uncertainty about design, certification, and air-traffic management considerations as altitude increases far above today's typical values; one example is the uncertainty associated with the design and weight prediction of high-altitude pressure vessels.

2.3 Formulation of an Optimization Problem Tailored to an Aircraft Configuration

After having selected the objective function (the performance metric), the reference aircraft, the mission variables, and the technology levels, an optimization problem can be formulated for each aircraft considered. To further ensure a fair comparison, the problems can be formulated using the same guiding principles with respect to the following four choices: 1) those design requirements and aircraft-design disciplines that are dominant contributors to the performance metric must be identified; 2) the appropriate physical-model fidelity levels must be determined such that reasonable accuracy is achieved at an acceptable computational cost; 3) appropriate design variables and constraints must be defined to enable an optimizer to realize the benefits of a configuration; and 4) the optimization problem structure must be determined, which is a configuration-dependent combination of physical models that ensures that the performance metric and the performance-based constraints can be cost-effectively and accurately calculated as a function of the design variables.

2.3.1 Critical Design Requirements and Aircraft-Design Disciplines

The number of critical design requirements enforced in complete aircraft design is large, and they stem from many interacting disciplines, each of which leads to potentially complex and computationally expensive physical models. However, each discipline contributes physical phenomena that differ in the significance of their eventual impact on the value of the performance metric. In many cases, the relevant disciplines are aerodynamics, structures, weight engineering, propulsion, and flight mechanics. Many physical models also capture interactions among aircraft-design disciplines, their multidisciplinary nature often being configuration-dependent. For instance, including the engine nacelles in the calculation of a static-margin design requirement, which renders necessary the coupling of an aerodynamics model and a propulsion model, may not substantially affect the relative performance-metric values. Moreover, this may be true for a CTW aircraft, but whether this is true for the tightly-integrated HWB aircraft is less clear, as this aircraft is more sensitive to (often multidisicplinary) physical effects that determine whether a given design requirement is met.

To reduce computational cost and complexity when comparing aircraft configurations in terms of a performance metric, aircraft models can therefore be constructed and optimized based only on critical design requirements and disciplines, *i.e.* those that have a significant effect on the value of the performance metric *relative* to that for the reference aircraft, while recognizing that the aircraft produced using such a distilled approach are not necessarily practical nor realistically feasible. Rather, the implicit premise is that the design changes that would be required to reach a certifiable aircraft design do not significantly affect relative aircraft performance as measured by the performance metric. These simplified optimization studies can also be used to complement aircraft design, as novel and efficient design features can thus be produced; this is especially true when considering large design spaces and high-fidelity physical models.

An aircraft must first be sized reasonably well before any performance metric or constraint can be accurately calculated. Depending on the selected design freedom, some sizing work can happen prior to optimization, during which the resulting aircraft components would be held fixed while those that depend on the design variables are sized, but in general, the critical design requirements form performance-based constraints that can be enforced through optimization. Many design requirements that have a significant effect on the performance metric can be determined by considering typical segments of a flight such as takeoff, low-speed flight, climb, and cruise [8, 9]. Descent may be of lesser importance, and, if takeoff and low-speed flight are considered, landing-performance targets may be achievable with adjustments that have a relatively inconsequential impact on the performance metric. Some edge-of-the-envelope considerations are also critical in sizing an aircraft, such as inoperative-engine directional trim at low speed, and structural integrity during a 2.5G pull-up; the latter is sometimes implicit in wing-weight models. Finally, depending on the aircraft configuration and the allowed design freedom, design requirements relevant to buffet and flutter avoidance may have only a negligible effect on relative performance.

To confirm that satisfying a given design requirement or including a given discipline indeed has a significant effect on relative performance-metric values, an optimization problem can be solved both with and without imposing this design requirement or including some discipline. If the change in relative performance-metric values is sufficiently small, the design requirement in question may be excluded in similar future cases to further reduce computational cost and complexity. However, engineering judgment is often required when selecting critical design requirements and disciplines, as testing every assumption is generally prohibitively expensive. Conservative but cost-saving assumptions can sometimes be made such that some mutually exclusive operating conditions are considered simultaneously, as fewer otherwise-identical design requirements thus need to be enforced. An example is enforcing a static-margin constraint with the aftmost center of gravity (CG) and at MTOW even though this combination may not occur simultaneously for a given aircraft.

2.3.2 Physical Model Formulation and Fidelity Levels

The critical design requirements are enforced as constraints in an optimization problem. Hence, physical models must be formulated (and evaluated) in order to determine whether the critical design

requirements are met, and to calculate the performance metric. As established in the previous section, when constructing the physical models it is important for efficiency to retain only those aircraft design disciplines that contribute physical phenomena that are significant in determining whether the critical design requirements are satisfied or that significantly contribute to calculating the performance metric.

Physical models vary in terms of their accuracy and sensitivity to variations in high-resolution details. Low-fidelity physical models capture general trends, are insensitive to high-resolution details, and are computationally inexpensive to evaluate, while high-fidelity models capture most of the relevant physical effects, depend strongly on high-resolution details, and are computationally expensive to evaluate. Medium-fidelity models lie between these two extremes. Due to recent progress in computational methods, medium- to high-fidelity models can now be incorporated earlier in the process of aircraft development, making the distinction between the classical conceptual-design and preliminary-design phases less obvious. This approach is key in accelerating the development of unconventional aircraft configurations for which few representative low-fidelity models exist. However, using high-fidelity models in optimization often involves some subtle risks and trade-offs like design-space multimodality [39], and convergence issues in high-dimensional design spaces [40]; therefore, they should only be used when doing otherwise would significantly impinge on the accuracy of the calculations.

It is possible to use a combination of low, medium, and high-fidelity physical models when calculating the performance metric and performance-based constraints if the physical quantities on which these depend are adequately captured by such a combination [17, 19, 21]. This leads to a multi-fidelity optimization problem. The key to determining the fidelity level needed for physical models whose outputs are used to accurately calculate the physical quantities that are dominant contributors to the performance metric, directly or through the design requirements, and to accurately capture the sensitivity of these physical quantities to the selected design variable types, is to determine whether they are mainly sensitive to the effects of simple or complex physical phenomena, and whether these sensitivities are due to low- or high-resolution design details. It can sometimes suffice to know only global aircraft dimensions or systems-level details. This can be the case for the estimation of various subsystem weights, for example. Low-fidelity models are adequate for such quantities, especially if they can reasonably be applied to each aircraft configuration considered. Otherwise, medium- to high-fidelity models can be used. For example, low-fidelity correlations are insufficient to model the dependence of the structure of complex unconventional wing systems, like a strut-braced wing, on the critical aerodynamic loads, but a medium-fidelity finite-beam-element model may be adequate. Moreover, the aerodynamic efficiency of an aircraft in transonic flight depends strongly on the precise shape of its outer mold line, which determines whether complex physical effects such as shock waves influence the performance metric. This suggests that a high-fidelity aerodynamics model is necessary to assess transonic aircraft performance. In general, some experimentation may be required to determine what fidelity level is needed for each relevant physical quantity, as the degree to which the performance metric depends on high-resolution design details or the effects of complex physical phenomena can be unclear. In a similar manner that testing whether some design requirements that are suspected to have a significant impact on relative performance-metric values indeed have such an impact, the fidelity level of certain physical models can also be varied and the corresponding impact measured.

2.3.3 Design Variables and Constraints

When selecting design variables to include in an optimization problem, one key requirement is that sufficient design freedom must be included in order to satisfy the critical design requirements. Many physical models relevant to aircraft design are a function of the internal or external geometry, so many aircraft components must be modeled with varying levels of geometric fidelity before analyzing or optimizing performance. The defining parameters of the geometric models can either be used directly as geometric design variables or first consolidated into parameters that can then be used as effective geometric design variables. The latter option is appropriate in the presence of high-fidelity

aerodynamics models that operate on an aircraft outer mold line, which may be parameterized by hundreds or thousands of variables. If these were used directly as design variables, their large number and the probable presence of nearly-redundant degrees of freedom could cause the optimizer to converge poorly and the design space could be excessively multimodal, resulting in unrealized performance potential [39, 40]. One option for consolidating the parameters is to define span, sweep, dihedral, chord, twist, and section-shape degrees of freedom, thus allowing an optimizer to adjust both global and local aspects of the geometry within a significantly reduced but adequately diverse design space [29]. This consolidation also facilitates enforcing constraints on these aircraft design parameters; however, the effective design variables do not need to represent typical or intuitive aircraft design parameters. The angle of attack is almost always included as a design variable, except for zero-sweep wing-only cases where it would be redundant with respect to twist design variables. Non-geometric design variables, such as altitude or engine size, can also be considered, but this is more case-dependent.

Enforcing linear constraints is one method of consolidating parameters into effective design variables, and both linear and nonlinear geometric constraints are often crucial in keeping optimal designs manufacturable (to avoid excessive wing waviness, for example). When enforced as performance-based constraints, the critical design requirements discussed previously indirectly restrict the design variables by implying bounds on component sizing, shaping, and positioning. In addition to multimodality, redundancy, and optimizer convergence issues, another risk inherent to poorly constrained optimization problems is physical-model exploitation. This occurs when an optimizer can realize a benefit by exploiting a limitation in a physical model. In general, some experimentation may be required to tailor the effective design variables and the constraints to the goals of an optimization study.

2.3.4 Optimization Problem Structure

Formulating an optimization problem requires coupling the disciplines through their physical models so that multidisciplinary effects are captured, thus providing the optimizer with the correct dependence of the required performance metric (objective function) and performance-based constraints on the design variables. All considered disciplines must be fully coupled in some optimization cases. This is recommended if the optimal value of many design variables is determined by multidisciplinary models spanning the full breadth of considered fidelity levels. Take an HWB aircraft for example: the optimal value of most geometric design variables depends strongly on transonic aerodynamic effects best captured through a high-fidelity aerodynamics model, but many are also strong determinants of pitch stability, which can be determined with a multidisciplinary model combining outputs from low-, medium-, and high-fidelity physical models. Therefore, a fully-coupled multifidelity multidisciplinary optimization framework is recommended for studying an HWB aircraft. Conversely, if the optimal value of many design variables depends strongly on multidisciplinary models that do not span the full breadth of fidelity levels, while the others depend in aggregate on only one or relatively few disciplines, it is often possible to reduce the cost of the optimization process by adopting a decoupled approach to aircraft optimization: A preliminary optimization problem akin to the conceptual-design phase of traditional aircraft design is first solved to determine the optimal values of those design variables with strong multidisciplinary dependencies that can be accurately captured with low- to medium-fidelity models. An optimization problem involving a high-fidelity models is then solved; it focuses on determining the optimal value of the remaining design variables, which are those with strong dependencies on one or relatively few disciplines that must be modeled with high-fidelity, such as aerodynamics. For example, low-fidelity aerodynamics and structural models can be used to size the empennage of a CTW aircraft, which would then be held fixed during the subsequent high-fidelity aerostructural optimization of the twist and section shapes of its wing.

In either the coupled or decoupled approaches, if a suitable estimate for the optimal value of a given design variable can be determined without recourse to optimization, perhaps by referencing studies of comparable aircraft found in the literature or through designer experience, then it can be held fixed from the beginning. This approach can be considered when some design variable is expected to depend strongly on difficult-to-model physical effects, such as flutter, or simply to target some subset

of the traditional geometric design variables.

3 Multifidelity Multidisciplinary Optimization Framework

This section reviews a specialized multifidelity multidisciplinary optimization framework that is well-suited to solve optimization problems formulated using the guiding principles discussed in Section 2. Section 3.1 covers the conceptual-design environment used in the first phase of the decoupled approach presented in Section 2.3.4. It is used to optimize a given aircraft with respect to those design variables that depend strongly on multidisciplinary effects that can be captured with low- to medium-fidelity physical models. Section 3.2 presents a high-fidelity aerodynamic shape optimization tool, which is used in the second phase of the decoupled approach to optimize the design variables that depend strongly on aerodynamics using a high-fidelity model; these remaining design variables are often wing twist angles and section shapes, and they are carefully constrained to maintain the feasibility of non-aerodynamics design requirements. Jetstream is also used as the backbone of the coupled approach, which is necessary when the optimal value of most design variables depends on multidisciplinary effects captured partly through high-fidelity aerodynamics models. Section 3.3 discusses how conceptual-design models are linked with the high-fidelity aerodynamic shape optimization tool for this purpose.

3.1 Conceptual-Design Environment

Faber is a conceptual design environment that can be used to develop aircraft concepts, which can serve as initial geometries for subsequent investigations involving optimization based on higher-fidelity physical models. To this end, a multidisciplinary optimization framework is built with mainly low-fidelity models to capture and enforce the design requirements that are most relevant to the overall sizing and feasibility of a given aircraft configuration, with performance targets defined based on a reference aircraft and representative nominal and sizing missions. The critical disciplines modeled are aerodynamics, weight engineering, structures, propulsion, and flight mechanics. Details on the physical models used are given in the following subsections. A nonlinear gradient-based optimization algorithm is used due to its relatively low computational cost when compared to global, gradient-free methods such as a genetic algorithm. Block fuel burn can be minimized, typically over the nominal mission, with respect to design variables that define the overall sizing of the wing, horizontal and vertical tails, and propulsion system. The initial cruise altitude of each mission can also be made free.

3.1.1 Aerodynamics

For aerodynamics, lift is set equal to weight at cruise and low-fidelity models are used to approximate viscous, induced, and wave drag. Contributions to induced and wave drag are modeled for the wing, with spanwise lift distributions assumed to be elliptical. Trim drag is assumed to be negligible. Viscous drag is calculated through the build-up method of Raymer [8], which includes approximations for skin-friction, form, interference, and excrescence drag from the wing, fuselage, horizontal and vertical tails, nacelles, and pylons. Boundary layers are assumed to be fully turbulent, although laminar flow approximations are also available. Induced drag is calculated through a vortex-lattice method coupled with a Trefftz-plane analysis, while wave drag is approximated through the sweep-corrected Korn equation [41].

3.1.2 Weight Engineering and Structures

The weight and CG of a given aircraft concept are approximated through the statistical correlations of Torenbeek [9], and Kroo and Shevell [42], respectively, for components that are assumed to be conventional. To capture the structural efficiency of unconventional wing systems, a medium-fidelity semi-empirical method is used, which implements a finite-beam-element structural sizing and analysis framework for estimating the weight of primary (structural) wing components [43]. Statistical correlations are used for secondary or non-structural wing components such as slats, flaps, spoilers, and ailerons, which are assumed to be conventional [44]. Secondary wing weight contributions also

include weight penalties from wing folding mechanisms, which provide the means for accommodating wing spans that exceed a given gate limit (*e.g.* 36.0 m (118 ft) for code-C gates). Fuselage bending loads due to the empennage are also captured by the empirical models, and a global buckling detection method is available for joined wing systems such as the strut-braced wing, whose wing segments can be subjected to compressive axial loads under certain loading conditions.

The fuel weights of an aircraft concept are calculated through the method of fuel fractions. Fuel fractions are included for 1) warm-up, taxi, and takeoff, 2) climb, 3) cruise, 4) descent, and 5) landing. For climb segments, an empirical relationship that depends on the initial cruise altitude of a mission is used. This ensures that the penalty in climb fuel for selecting high cruise altitudes is approximately captured. For cruise segments, the Breguet range equation is used. It assumes a steady cruise-climb profile at constant Mach number and lift coefficient.

3.1.3 Propulsion

The propulsion model provides a means for scaling the propulsion system as the thrust requirements of the aircraft concept evolve. The rubber engine model of Gur et al. [45] is used to resize the weight and performance of a reference engine based on thrust requirements. A linear parametric model is also included to scale the dimensions of a reference nacelle and pylon system with changes in the thrust requirements.

3.1.4 Flight Mechanics

The conceptual-design environment assumes that aircraft can be maneuvered with conventional control surfaces, that their empennage can be resized to make up for any losses in stability-and-control (S&C) performance while having little impact on the performance metric, and that roll authority can be tuned to desired values later in the design process. The static margin can be estimated using the DATCOM method [46]. In this work, aircraft with more unconventional S&C characteristics, like the HWB, are not analyzed and optimized with Faber, so more complex S&C models are not needed here. Since takeoff and landing are not explicitly modeled in Faber, nonlinear constraints can be introduced to place an upper and lower bound on the design wing loading and thrust-to-weight ratio, respectively. Other nonlinear constraints often include minimum tail volume ratios for sizing the horizontal and vertical tails, and minimum top-of-climb excess thrust requirements to ensure that the propulsion system can generate sufficient thrust at all relevant cruise altitudes, with the top-of-climb rate-of-climb being calculated through a force balance.

3.2 High-Fidelity Aerodynamic Shape Optimization Framework

The high-fidelity aerodynamic shape optimization framework Jetstream, which has been developed at the University of Toronto Institute for Aerospace Studies [10, 12, 24, 29, 40], is used in this work. It consists of three main components: 1) a method for geometry parameterization and control with integrated grid deformation, 2) a solver for the Reynolds-averaged Navier-Stokes (RANS) equations, and 3) adjoint-based flow-dependent gradient computations with optimization performed using a third-party optimizer. This aerodynamic shape optimization framework has been verified through the AIAA Aerodynamic Design Optimization Discussion Group [47, 48] and by direct cross-validation with an industrial code [49]. Its three main components are described below.

3.2.1 Geometry Parameterization and Control with Integrated Grid Deformation

The geometry is parameterized by B-spline surfaces, the control points of which are embedded in free-form deformation (FFD) B-spline volumes to make the geometry control system independent of the surface parameterization. The control points of the FFD volumes are grouped into intuitive geometric parameters, namely twist angle, chord length, and section shape. The control points of embedded *axial curves* govern the span, sweep, and dihedral. The two sets of control points serve as the geometric design variables during high-fidelity aerodynamic shape optimization [29]. In addition to the surface being parameterized with B-spline patches, each block of the multiblock CFD grid is itself parameterized with a B-spline volume. The control points of these B-spline volumes form a

lattice that is used to formulate a linear-elastic finite-element problem. This problem is solved to obtain the deformed B-spline volume control grid based on the propagation of surface changes before the deformed volume grid is algebraically regenerated [10]. This provides a robust grid deformation strategy which is generally capable of maintaining grid quality even after large shape changes. The FFD volumes can also be used to deform the trailing edge to model control-surface deflections. To accomplish this, the FFD control points aft of a specified hinge line on target cross-sections rotate about that hinge line, thus imparting a continuous-mold-line control-surface-like deflection to the aircraft surface [17].

3.2.2 RANS Flow Solver and Spatial Discretization

Clean airframe drag is calculated using a parallel implicit multiblock solver for the RANS equations that is closed with the negative variant of the Spalart-Allmaras turbulence model. The solver has been validated during the 5th AIAA Drag Prediction Workshop [50]. Second-order summation-by-parts operators are used for spatial discretization, and simultaneous approximation terms impose boundary and block-interface conditions [10]. The grids used for optimization must effectively balance accuracy and computational cost, while predicting with reasonable accuracy the relative contributions of all components of clean-airframe drag. Obtaining practical turn-around times for optimization often necessitates relatively coarse grids, but correction factors can be used to approximately account for the discretization error during optimization to better estimate fuel quantities in the coupled approach to optimization. Care must be taken to ensure that the relevant flow features, such as shocks and separation, are captured, so that design changes are correctly informed. To measure the performance of optimized geometries, grid-convergence studies are conducted post-optimization to reduce numerical errors well below what is seen on the optimization-level grid.

3.2.3 Optimization Algorithm and Flow-Dependent Gradient Evaluation

The high cost of evaluating the flow-dependent objective function and constraints motivates the use of an efficient gradient-based algorithm. The Sparse Nonlinear Optimizer (SNOPT) gradient-based optimization algorithm is used for its ability to efficiently solve large-scale constrained problems. The optimizer uses sequential quadratic programming and approximates Hessian matrices with the method of Broyden, Fletcher, Goldfarb, and Shanno, as described in Ref. [51].

Accurate gradients are required to converge the optimization problem. Due to the large number of design variables relative to the number of required gradients, flow-dependent gradients are evaluated using the discrete adjoint method. All necessary partial derivatives are obtained by analytical or complex-step differentiation of the geometry control, grid deformation, and flow solvers described above. The resulting adjoint system is solved to a relatively tight tolerance (10^{-8}) with a simplified and flexible version of the generalized conjugate residual with orthogonalization and truncation (GCROT) algorithm [52] in about one-third of the time required for a flow solution. Details pertaining to the implementation of the discrete adjoint method are given in Refs. [10, 12].

3.3 Multifidelity Multidisciplinary Aircraft Design Toolbox

For the coupled approach to aircraft optimization, a multifidelity multidisciplinary toolbox is available for modeling and coupling non-aerodynamics disciplines with the high-fidelity aerodynamic shape optimization framework described in Section 3.2. Further details can be found in Reist *et al*. [17], and the main ideas are summarized below.

3.3.1 Aerodynamics

To more accurately calculate fuel weight, the clean-airframe drag calculated using the RANS solver is augmented with low-fidelity relations for excrescence, nacelle, and windmilling drag, the latter only being relevant when analyzing one-engine-inoperative (OEI) design requirements [8]. Aerodynamic interactions between the nacelles and the outer mold line are neglected. Ground effect is modeled for on-ground analyses by enforcing a tangential velocity at a nearby ground plane.

3.3.2 Weight Engineering and Structures

The weight of aircraft components that are approximately conventional are calculated using the statistical correlations of Torenbeek [9]. For example, the wing-weight model depends on geometric parameters including the span, area, root thickness, and sweep angle of the wing proper, *i.e.* without considering the offset provided by a fuselage or the centerbody of an HWB aircraft. The weights of unmodeled aircraft subsystems (termed fixed weights) are precalculated, and fuel weights are estimated through the fuel-fractions method described in Section 3.1. Used especially in HWB cases, this toolbox contains an HWB-specific model that gives the centerbody weight mainly as a function of the pressurized and unpressurized projected centerbody areas [53]. The proportion of the total lift carried by the wing also enters into the sizing of HWB aircraft, and the weight of winglets or fins is provided through an empirical correlation with their wetted area.

The CG and mass-moment of inertia about the lateral axis are calculated based on the high-fidelity outer mold line geometry with a few assumptions. Namely, it is assumed that the structural mass distribution is homogeneous within the shell of the airframe, that engines are point-masses, that the fuel weight acts through the wing volume centroid, and that the fixed weights act through the shell centroid of the fuselage or centerbody. Specifically for the HWB, the payload weight acts at the volume centroid of a polyhedron enclosing the cockpit, cabin, and cargo holds, and the weight of the two rear-mounted engines acts one nacelle diameter upstream of the centerline trailing edge.

3.3.3 Propulsion

All engine characteristics are scaled based on the critical maximum thrust requirement using a rubber-engine model similar to that discussed in Section 3.1. Namely, this model gives the takeoff and cruise thrust, weight, thrust-specific fuel consumption, and nacelle length and diameter, based on a specified reference engine.

3.3.4 Flight Mechanics

Multifidelity flight-mechanics models are formulated based on the outputs of the aerodynamics, structures, weight-engineering, and propulsion models. Constraints are formulated based on static S&C models, such as trimming using the continuous-mold-line control-surface approximations, or calculating the initial angular acceleration produced by control-surface deflections. Aerodynamic derivatives are approximated through finite differences based on high-fidelity aerodynamics data for use in, for example, the calculation of static margin. A multifidelity model for takeoff field length is also available, and it relies on aerodynamics data from on-ground performance analyses and a medium-fidelity dynamical model applied between the start of the ground-roll up to the takeoff screen height of 10.7 m (35.0 ft). Finally, a force-balance-based top-of-climb rate-of-climb model can be used to place a lower bound on engine size if a constraint on the takeoff field length is not critical.

4 Application to the Assessment of Regional-Class SBW and HWB Aircraft

In this section, problem formulations developed by applying the guiding principles discussed in Section 2 and the methodologies presented in Section 3 to a reference CTW aircraft and two unconventional aircraft, the SBW and HWB, are presented. This work seeks to quantify any inherent benefit that these unconventional configurations may confer to regional-class aircraft designed with current technology levels. Regarding the selection of a performance metric, block fuel burn is particularly relevant for regional-class aircraft because they spend large proportions of their short-range missions in climb. Regarding the selection of mission variables, a 500-nmi (926-km) nominal mission is defined and flown at Mach 0.78, and the payload corresponds to 104 passengers (10 380 kg, or 22 880 lb). The aircraft are sized for a 3100-nmi (5 741-km) design mission. The fuel required for any given mission is carried along with that required for a 45-min loiter at an altitude of 4 572 m (15 000 ft) and a 100-nmi (185-km) diversion during which the same low cruise altitude is reached. Many of the above values are based on the Embraer E190-E2, which is selected to represent a modern best-in-class CTW regional jet.

As a result of their nature, each aircraft configuration leads to differences in the critical design requirements and disciplines and the associated physical models and fidelity levels, the design variables and constraints, and the structure of the resulting optimization problems, as discussed below. Nonetheless, there are several similarities between the optimization problems. Namely, optimization based on high-fidelity aerodynamics models is required in every case, thus requiring high-resolution models of the outer mold line. For the CTW and SBW, the wing system, fuselage, and tailplane are modeled. This is the minimum number of aircraft components required to capture the dominant aerodynamic effects, including the lift produced by the fuselage, the trim drag from the horizontal tail, and the interference effects at junctions. For the HWB, a model of the centerbody, transition region, wing, and winglets is optimized. This model includes all components of the outer mold line except those of the engine group, and it makes use of the continuous-mold-line control-surface model, as the HWB is a tightly-coupled aircraft configuration whose performance is affected by many off-design performance requirements.

4.1 Conventional Tube-and-Wing Aircraft

The regional-class CTW aircraft that serves as a performance baseline in this work is referred to as the CTW100. Modeled after the existing Embraer E190-E2, many elements of its design can be taken from the existing reference aircraft and frozen, giving rise to an “as-drawn” CTW reference aircraft consistent with Option 1 discussed in Section 2.2. The fuselage geometry, wing planform, engine locations, and empennage are not designed here; rather, the design tools presented in Sections 3.1 and 3.2 are used to derive the characteristics and performance of the existing reference aircraft. The wing sections are not publicly available and are difficult to extract from three-view aircraft drawings; hence, they are primarily designed through high-fidelity aerodynamic shape optimization. The decoupled, two-phase approach discussed in Section 2.3.4 is appropriate for a CTW aircraft. Conceptual-level models are well-suited to its basic sizing and analysis, but a second phase, consisting of high-fidelity aerodynamic shape optimization, can be useful even when considering an as-drawn aircraft. This ensures that the performance assessment is consistent with that of the unconventional aircraft, and that a credible estimate of the performance of the real reference aircraft can be obtained. Both phases of the decoupled approach to the optimization of the reference CTW aircraft are further discussed below.

4.1.1 Phase One: CTW100 Conceptual-Design Problem Formulation

For the reference CTW aircraft, two sizing missions on the MTOW-limited section of the payload-range curve are analyzed. The first consists of flying 2 150 nmi (3 982 km) from MTOW with the maximum payload, and the second consists of flying 3 400 nmi (6 297 km) from MTOW with full fuel tanks. This approach results in a closer match to the payload-range diagram of the existing reference aircraft than only analyzing the design mission. The cruise altitude of all missions is 11 280 m (37 000 ft), which is typical of the reference aircraft.

The wing and tail planform and other global dimensions are modeled directly from the data provided in the airport planning manual [54], and the propulsion model is tuned to represent the Pratt & Whitney PW1919G engine [55]. In Phase One, the conceptual-design environment is used to determine the minimum required wing thickness-to-chord ratios, which are essentially thickness design variables when chord length is fixed. For consistency with the SBW aircraft, the wing is analyzed using the medium-fidelity finite-beam-element model, although this is not strictly necessary for the CTW100 for which adequate low-fidelity models exist. The most critical of the two sizing missions sizes the wing structure, with a 2.5G load and a -1.0G load being applied based on the lift required at cruise for that mission. For weight and balance, the conceptual-level models described in Section 3.1 are deemed sufficiently accurate.

The objective for Phase One is to minimize block fuel burn over the nominal mission, while subject to the wing structure sizing constraints discussed above and a minimum constraint on the wing volume based on the fuel required to complete the most fuel-critical sizing mission. Results indicate that the design weights of the aircraft are in close agreement with those of the Embraer E190-E2 [54];

Table 1 – CTW100: Design variable information for high-fidelity aerodynamic shape optimization.

Design Variable	Quantity	Bounds
Angle of attack	1	$\pm$ 3^o
Wing twist angle	12	$\pm$ 10^o
Horizontal tail incidence angle	1	$\pm$ 10^o
Section shape	264	0.5 to 2.0 [1]
Total	**278**	–

[1] Expressed as a multiplier of the initial local vertical coordinate.

see Section 5.1, although calibrations to the empirical models are introduced to achieve this. These calibrations are carried over to the sizing of the unconventional aircraft for consistency.

4.1.2 Phase Two: CTW100 High-Fidelity Aerodynamic Shape Optimization Problem Formulation

Due to the nonlinear nature of the flow at transonic Mach numbers as well as viscous effects, RANS-based aerodynamic shape optimization is needed during high-fidelity aerodynamic shape optimization for the accurate determination of fine-resolution design aspects that are significant determinants of aerodynamic performance. The outer mold line model of the CTW100 is created based on the aircraft concept developed in Phase One, and the design aspects that have a strong effect on non-aerodynamics disciplines are held fixed. Thus, the design variables are the angle of attack, as well as the twist angles and section shapes at multiple stations across the wing. The incidence angle of the tail is also free to ensure pitch trim through a nonlinear constraint. The design variables and their bounds are summarized in Table 1. Other nonlinear constraints include a trimmed lift coefficient, minimum wing volume to accommodate the fuel tanks sized by Faber, and lower bounds on the maximum sectional thickness-to-chord ratios across the wing to serve as surrogates for maintaining the minimum bending stiffness distribution provided by Faber.

The objective function for the high-fidelity aerodynamic shape optimization is to minimize drag at the start of cruise for the nominal mission. This is equivalent to minimizing block fuel burn when altitude is fixed, the design variables have only a small effect on structural weight, and the fuel weights are acceptably well estimated by Faber. Indeed, if those assumptions hold true, the contributions to block fuel burn from takeoff, climb, descent, and landing can be assumed constant, and so can the engine size, so the only remaining factor in determining block fuel burn is cruise drag.

4.2 Strut-Braced-Wing Aircraft

The SBW aircraft derives its main aerodynamic advantage from its high-aspect-ratio wing, whose high span is enabled by the supporting strut, allowing for a substantial reduction in induced drag when compared to a conventional cantilever wing [56–59]. The structural efficiency provided by the strut also enables thinner wings, thus reducing form and wave drag, and wing weight (and thus induced drag). With regard to wave drag, the reduced thickness also increases the critical Mach number, which can allow for reduced wing sweep, also helping to reduce wing weight. The design of the wing-strut junction poses a challenge for wave-drag reduction and boundary-layer separation. The transonic-channel effect in the region between the wing, strut, and fuselage can also be challenging to mitigate. Due to its high aspect ratio, the SBW aircraft performs better at altitudes higher than those at which current CTW aircraft operate [4], which can pose a challenge for air traffic management and aircraft certification.

The SBW aircraft is similar to a CTW aircraft in many regards: it has a cylindrical fuselage, and it had a classical empennage for pitch and yaw stability and control (S&C). For this reason, many design variables can be optimized using conceptual-level models, making the decoupled approach described in Section 2.3.4 appropriate once again. Thus, the regional-class SBW aircraft, referred to

as the SBW100, is first designed using Faber in Phase One, and the aircraft concept thus obtained is then refined in Phase Two using the high-fidelity aerodynamic shape optimization code Jetstream. Block fuel burn is then calculated.

4.2.1 Phase One: SBW100 Conceptual-Design Problem Formulation

The SBW100 is first developed through the application of conceptual-level multidisciplinary optimization. As for the CTW100, the design weights of the aircraft are largely determined by the requirements of the two sizing missions (maximum-payload and maximum-fuel missions), while the nominal mission is used to estimate block fuel burn. Many conceptual-design tools are appropriate; however, the medium-fidelity beam-element finite-element model is necessary for wing structural analysis and weight estimation due to the presence of the strut. Composite wing structures are assumed to be a current technology, and thus are adopted for the wing system of the SBW100. The statistical correlations also account for the fuselage-weight penalties associated with the high-wing configuration of the SBW100, as well as those that come from having a fuselage-mounted landing gear system. Due to the relatively decoupled nature of the SBW aircraft, off-design conditions, such as takeoff, low speed trim at CG extremes, and low-speed one-engine-inoperative performance, can be neglected, as the control surfaces, high-lift devices, and empennage can be assumed to satisfy these off-design requirements if they are sized similarly to those of the CTW. Thus, analyzing only cruise performance is again sufficient. The selected reference engine is the Pratt & Whitney PW1919G [55], with the nacelles and pylons modeled based on those of the Embraer E190-E2. This engine is scaled based on the thrust requirements of the SBW100, unlike for the CTW100 for which the reference engine is modeled as-drawn.

The mission variables are the same as those for the CTW100 except two initial cruise altitudes, which are design variables. One applies to the two sizing missions and the other to the nominal mission. The two altitude design variables provide the optimizer with a means of better realizing the potential of the high-aspect-ratio wings. To ensure that these design variables are sufficiently constrained, a minimum bound is placed on the top-of-climb thrust of the propulsion system to ensure that it can produce a 1.52-m/s (300-ft/min) rate of climb. Constraints are also introduced based on the buffet heuristics presented in Chau and Zingg [21]. These place a more stringent check on wave drag when considering operating conditions along a notional buffet envelope, which may be encroached upon when operating at high cruise lift coefficients.

The objective of the conceptual-level multidisciplinary optimization problem is again to minimize block fuel burn for the nominal mission. The design variables help size the wing, strut, horizontal and vertical tails, and propulsion systems, and optimize the initial cruise altitudes. For the wing and strut, the design variables are the chord and thickness-to-chord ratio that define three segments for the wing (*i.e.* the carry-through, inboard, and outboard wing segments) and three segments for the strut (*i.e.* the carry-through, main, and vertical strut segments). Some design variables such as wing span, wing sweep, and the strut attachment locations have been removed from the design space, as they have been set while considering multiple design requirements that are not modeled in Faber by variants of the Boeing SUGAR High [60]. This is a conservative approach that avoids the need to model effects like flutter, which may be especially relevant for this high-aspect-ratio wing. Due to fixing these design variables, the wing area is primarily sized through chord lengths and bound by a constraint on the maximum wing loading based on the Embraer E190-E2, *i.e.* an upper bound of 5.28 kN/m^2 (110 lb/ft^2). This is paired with a minimum design thrust-to-weight ratio constraint that drives a design variable for the maximum thrust requirement of the aircraft. The minimum bound is taken to be 0.336, which is also based on the Embraer E190-E2. These constraints help ensure that takeoff and landing requirements are approximately met, while avoiding the need to explicitly model low-speed aerodynamics. The design variables for the horizontal and vertical tails are the root and tip chord lengths, as well as the streamwise attachment location of the vertical tail and the streamwise and vertical attachment locations of the horizontal tail, which are constrained to maintain the initial relative arrangement of the T-tail of the Boeing SUGAR High [60]. The sizing of the horizontal and vertical tails is driven by minimum tail volume ratio constraints, as well as constraints that maintain

Table 2 – SBW100: Design variable information for high-fidelity aerodynamic shape optimization.

Design Variable	Quantity	Bounds
Angle of attack	1	$\pm$ 3^o
Wing and strut twist angle [1]	38	$\pm$ 10^o
Horizontal tail incidence angle	1	$\pm$ 10^o
Wing and strut section shape	836	0.5 to 2.0 [2]
Total	**876**	–

[1] Wing-root and vertical-strut twist bounds are limited to $\pm$ 3.5 deg.

[2] Expressed as a multiplier of the initial local vertical coordinate.

constant taper and aspect ratios. Again, a constraint on the minimum wing volume ensures proper fuel-tank sizing, but for the SBW100, the fuel tanks are considered to reside within both the wing and strut.

4.2.2 Phase Two: SBW100 High-Fidelity Aerodynamic Shape Optimization Problem Formulation

In addition to the goal of refining the estimates of aerodynamic performance and credibly estimating block fuel burn, for the SBW100 aircraft, another goal of high-fidelity aerodynamic shape optimization is to determine how best to address the aerodynamic challenges in the region between the wing and the strut. The RANS equations are especially crucial in this regard, as they accurately capture all forms of cruise drag, including the transonic interference effects in and around the wing-strut junction. As with the CTW100, a model of the outer mold line of the wing and strut, fuselage, and tailplane is created based on the aircraft concept developed in Phase One, and the design aspects that have a strong effect on non-aerodynamics disciplines are held fixed. Thus, the design variables include the angle of attack, wing twist angles and section shapes, and the incidence angle of the horizontal tail for pitch trim. Specifically for the SBW100, the twist angle and section shape at several stations across the strut are also designed, the fuel-volume constraint corresponds to the wing and strut internal volume, and lower bounds on the strut-section thicknesses are transferred from Faber (along with those for the wing). Moreover, other geometric constraints are included to help maintain the manufacturing practicality of the wing and strut shapes, *e.g.* constraints that prevent excessive waviness near the wing-strut junction. The design variables and their bounds are summarized in Table 2. Again, the objective of the optimization is to minimize drag at the start of cruise for the nominal mission, and a trimmed lift coefficient is required. Although there are significantly more design variables in this case, many are concentrated around the wing-strut junction in order to give the optimizer ample freedom to design this critical region of the aircraft.

4.3 Hybrid-Wing-Body Aircraft – HWB100 Multifidelity Multidisciplinary Optimization Problem Formulation

The HWB achieves its aerodynamic efficiency from its large span and low wetted area [61]. The large span is enabled, without a prohibitive increase in wing weight, by the large width of the thick centerbody, which effectively offsets the wing root laterally, giving a larger total span for a given "wing-only" span. The lifting centerbody also reduces the lift that must be carried by the wing, and the configuration tends to be more spanloaded than a CTW, both effects acting to reduce the net wing bending loads. A reduction in wetted area comes from the incorporation of the fuselage into the lifting surface, as well as the elimination of the empennage. The combination of the effects discussed above increases the wetted aspect ratio, which is directly correlated with the lift-to-drag ratio. The challenges of this configuration stem primarily from the design of a low-weight centerbody structure that can efficiently support the internal pressure loads, the satisfaction of S&C requirements without an empennage, and the design of an efficient multifunctional aerodynamic shape under many

performance-based constraints.

The tightly integrated nature of the HWB makes the decoupled optimization procedure that was used for the CTW and SBW insufficient; therefore, the HWB100 is optimized with the coupled multifidelity multidisciplinary framework discussed in Section 3.3. For an HWB aircraft, S&C requirements are relatively highly dependent on the planform. Unlike for the CTW or SBW aircraft, the specification of the wing location and an appropriately-sized empennage cannot be relied upon to satisfy S&C constraints, so design features that significantly affect block-fuel-burn are sometimes needed; however, a high-fidelity aerodynamic shape optimization framework can help mitigate these penalties [17, 19]. For example, producing a sufficient pitching moment for takeoff is particularly difficult, as the pitch control surfaces are located relatively close to the main landing gear. However, DZYNE Technologies has recently patented a variable-length landing gear system known as the pivot-piston, which is actuated by the downforce created by upward-deflected pitch effectors, as opposed to a pitching moment about the main landing gear axles, to achieve rotation for takeoff [62, 63]. This technology effectively decouples the planform from the S&C design requirement of rotating for takeoff. In other regards, the planform also helps determine the location and size of the vertical surfaces, whether they be centerbody-mounted fins or large winglets, which are used to satisfy directional S&C design requirements.

The coupled multifidelity multidisciplinary optimization approach simultaneously considers the disciplines of aerodynamics, structures, weight engineering, propulsion, and flight mechanics. As with the CTW and SBW aircraft, a high-fidelity aerodynamics model is needed to ensure accurate aerodynamic analysis and design optimization. Since the wing of an HWB is cantilevered, the low-fidelity weight models discussed in Section 3.3 are used for weight prediction, although the precise location of the wing root is more difficult to identify due to the blending. Nonetheless, conceptual-level models that are functions of the planform geometry and wing loading are assumed to be sufficient for approximately capturing the trade-offs associated with changes in the wing planform. The S&C design requirements depend on the CG and moments of inertia, so these quantities are calculated as described in Section 3.3.2. The continuous-mold-line approximations of control surfaces are included in the high-fidelity aerodynamics model for use in trimming and controllability constraints. The rubber engine model described in Section 3.3.3 is used to resize a reference engine based on maximum thrust requirements either at the top of climb or during takeoff. Finally, the same fuel fraction method used for the CTW and SBW aircraft is used to calculate fuel weights, with drag correction factors based on a grid-convergence study on an intermediate geometry being used to account for the discretization errors that arise on the relatively coarse optimization-level grid.

Block fuel burn is minimized for the nominal mission with drag evaluated at the start of cruise. Performance is evaluated on the nominal mission, and the aircraft is sized based on the design mission, as opposed to both the maximum-payload and maximum-fuel missions used during Phase One of the CTW and SBW aircraft optimizations. This cost-saving measure was adopted since the HWB100 is sized using a high-fidelity aerodynamics model, as opposed to the CTW100 and SBW100, which are sized with conceptual-level models. Similar predictions of block fuel burn are expected at reduced cost for the following two reasons: First, the maximum-payload, maximum-fuel, and design missions are all located on the MTOW-limited portion of the payload-range curve. Second, despite the slight underprediction of the maximum fuel weight that results from not considering the maximum-fuel mission, the square-cube law suggests that even a moderate increase in the fuel tank volume (wing volume) would produce only a relatively small increase in wing surface area and thickness, and hence parasitic drag. The validity of the assumption that this approach results in similar block fuel burn predictions could be verified in future work.

The need to evaluate performance during both the nominal mission and the design mission leads to the definition of two sets of operating conditions, or analysis points, which are the following:

1. The start of cruise for the nominal mission described at the start of Section 4;
2. The start of cruise for the design mission described at the start of Section 4.

In addition, performance-based constraints enforced at the three following off-design analysis points

have been determined to have significant effects on the performance and block fuel burn of regional-class HWB aircraft [17, 19]:

3. Mach-0.20 low-speed flight (near liftoff speed, V_{LO}) at MTOW, at sea level, with an aft CG, and with low thrust;
4. Ground-roll at the on-ground minimum control speed, V_{MCG} (approximately Mach 0.15), with one engine inoperative;
5. Ground-roll at rotation speed, V_R (approximately Mach 0.20), with full thrust and the most critical combination of weight and CG.

Regarding constraints, the aircraft is required to be trimmed while using the pitch effectors at the nominal-mission analysis point, but these are not free to assist with trimming at the design-mission analysis point, as it is selected as their datum in this case. Trim and static margin constraints are imposed at Analysis Point 3, where the pitch effectors can assist with constraint satisfaction. The aircraft can be slightly statically unstable, with the lower bound on the static margin set to -4.0% MAC. This relaxed stability improves performance, and it is deemed allowable because stability augmentation software is assumed to be certifiable by the time HWB aircraft enter into service. Moreover, the block fuel burn of CTW and SBW aircraft is relatively insensitive to a static margin constraint. At analysis point 4, directional trim must be achieved using winglet-mounted rudders at the target on-ground minimum control speed with one engine inoperative. As per Reist *et al.* [17], the low speed makes this condition more critical from the perspective of sizing the winglets and the rudders than crosswind flight. The same study showed that large winglets offer similar performance to centerbody-mounted fins, so only the former configuration was studied here. Analysis Point 5 is used to impose a constraint on the initial pitch acceleration produced by partial deflection of the pitch effectors at rotation speed under the most critical weight-CG combination; the lower bound is set to $3\,\mathrm{deg/s^2}$. In this paper, Analysis Point 5 is both included and excluded in two otherwise identical optimization problems to demonstrate that removing a given constraint reveals whether the corresponding design requirement indeed has a significant effect on the performance metric. Moreover, removing the rotation constraint supports the case for full reliance on variable-length landing gear, which is an enabling technology at least for regional-class HWB aircraft [62, 63]. This does not introduce unfairness, as initiating rotation is not expected to be significantly punitive, if at all, for CTW and SBW aircraft given the long moment arm of their horizontal tail with respect to the main landing gear axles. Both on-ground analysis points model ground effect by enforcing flow tangency at the ground plane. The aerodynamic performance at the OEI and low-speed-flight analysis points (3 and 4) is reused in a medium-fidelity takeoff field length model that calculates the accelerate-go and accelerate-stop distances as a function of the engine-failure speed, the rotation speed, the all-engines-operational (AEO) and OEI liftoff speeds, and the AEO and OEI airborne times up to the 10.7-m (35.0-ft) takeoff screen height. These quantities are all design variables except the rotation speed when variable-length landing gear is not assumed to be available. The target balanced field length is 1 650 m, which is approximately that of the Embraer E190-E2 at sea-level. This takeoff-field-length constraint sizes the engine when the top-of-climb rate-of-climb requirement of 1.52 m/s (300 ft/min) is not critical. Other takeoff constraints include a steady-climb-speed safety margin to stall of 1.13, and an OEI-climb-angle lower bound of 1.37^o following liftoff.

The geometric constraints imposed on the HWB100 are that its wings are sufficiently voluminous to carry the required fuel for the design mission, that the cockpit and cabin be enclosed within the outer mold line of the centerbody and that the adjacent cargo holds fit within the transition region, and that the wingtips be protected from ground strikes up to simultaneous pitch and roll attitudes of 9^o and 9.5^o. The latter constraint has the most significant impact on wing dihedral in these cases, and it can act to inhibit excessive growth in wing span, although this does not occur here. The centerbody planform is largely constrained by the specified cabin-polyhedron, which keeps the centerbody weight model within its range of validity. Reasonable wing thicknesses are encouraged by the fuel-volume constraint and ensured by lower bounds on the section-shape design variables that keep the wing thickness-to-chord ratios above 9.6% at the root and 8.0% at the tip. The validity of this approach

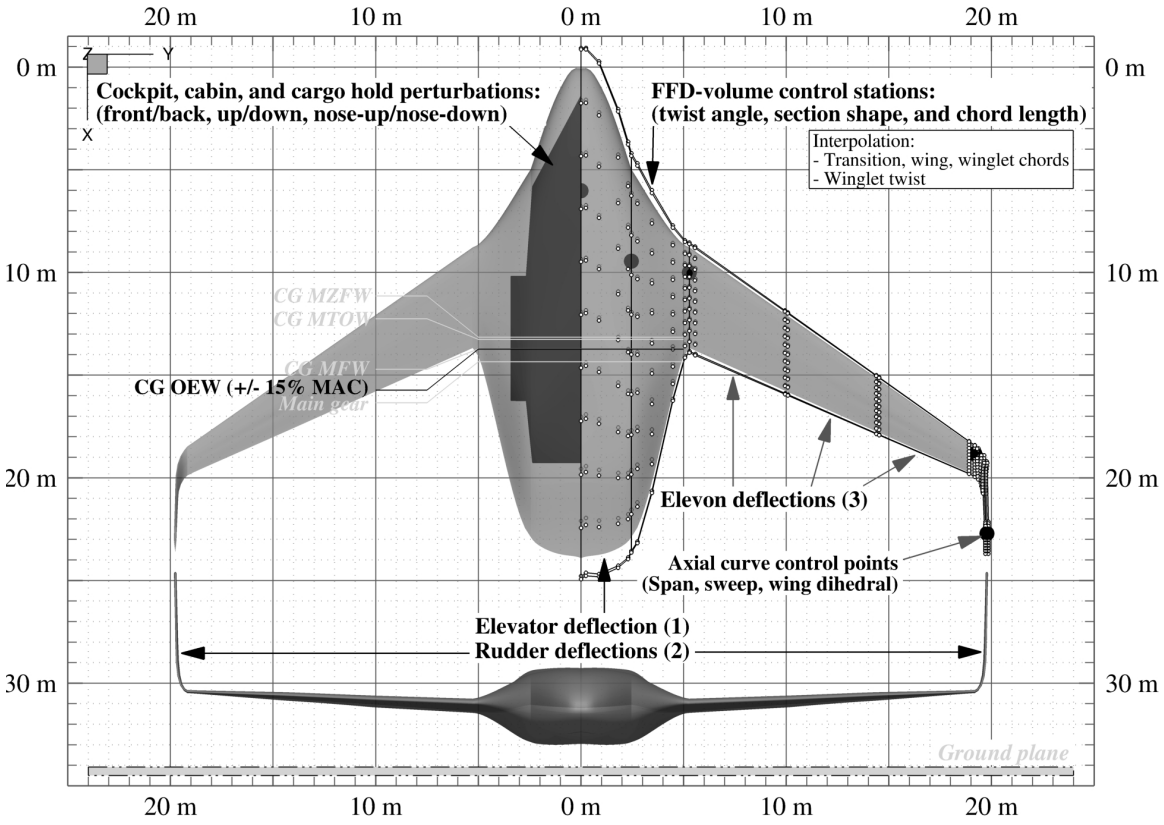

Figure 1 – HWB100: Visualization of some design variables and other problem information on a sample HWB-aircraft geometry.

could be verified with a sturctural model, but relative block-fuel-burn values are not expected to be significantly affected.

The initial cruise altitude was parametrically varied, with optimization problems solved at 10 970 m (36 000 ft), 12 190 m (40 000 ft), and 13 410 m (44 000 ft). The design variables include the cruise and low-speed angles of attack, the deflection angles of the two winglet-mounted rudders, one centerbody-mounted elevator, and three independent elevons, the position and orientation of the cabin-polyhedron, the six takeoff variables discussed above, the engine sea-level-static thrust multiplier, and the freedom to perturb the calculated structural (OEW) CG by $\pm$ 15% MAC to account for unconsidered CG placement strategies that could be envisaged during more advanced design work. The spans and sweep angles of the four major aircraft regions (centerbody, transition region, wing, and winglet), and the wing dihedral angle, are controlled by the axial curves, while the twist angles, chord lengths, and section shapes are controlled at multiple spanwise stations by the FFD-volume control points; these are the geometric design variables. The locations of the FFD-volume control points, which are arranged into control stations, and the axial curve control points, are shown in Figure 1. Many FFD-based design variables are allowed to vary nonlinearly across the span, with the only linearly-interpolated variables being the transition-, wing- and winglet-interior chord lengths, and the winglet-interior twist angles. Such design-variable linking prevents impractically wavy geometries from being produced, thus enhancing manufacturability. Future studies could incorporate simply-curved leading and trailing edges to further increase geometric freedom. Nonlinear spanwise variation in twist angles and section shapes is crucial to enable the full potential of the configuration to be achieved [19]. Additional information on the design variables can be found in Table 3.

5 Results

This section presents and discusses the results obtained by solving the optimization problems formulated in Section 4, which estimate the relative performance of each configuration in terms of the

Table 3 – HWB100: Design variable information for multifidelity multidisciplinary optimization.

Design Variable	Quantity					Select bounds				
Analysis point →	1	2	3	4	5	1	2	3	4	5
Angle of attack	1	1	-	-	1	-[1]	-[1]	-	-	-
Elevator deflection	1	-	-	1	1	$\pm 20^o$	-	-	$\pm 20^o$	$\pm 20^o$
Elevon deflection	3	-	-	3	3	$\pm 12.5^o$	-	-	$\pm 12.5^o$	$\pm 12.5^o$
Rudder deflection	-	-	2	-	-	-	-	$\pm 30^o$	-	-
Twist angle			13							
Section shape			360			$t/c \geq 9.6\%$ (wing root)				
Chord length			7			Wingtip: 1.52 m, Winglet tip: 0.91 m				
Region spans			4							
Region sweep angles			4							
Wing dihedral angle			1							
Cabin perturbation			3			$-2.5^o \leq \theta_{cabin} + \alpha \leq 2.5^o$ [1]				
OEW CG perturbation			1			$\pm$ 15% MAC				
Thrust angle			1			$\pm$ 15°				
Maximum thrust scaling			1							
Takeoff field length [2]			6			V_R = 68.2 m/s (Mach 0.20) [3]				
Total			**418**							

[1] The angle of attack is not limited, but the cabin floor angle must be within $\pm$ 2.5° at cruise.

[2] A function of engine-failure speed, rotation speed, all-engines-operational (AEO) and one-engine-inoperative (OEI) liftoff speeds, and AEO and OEI airborne times up to the 10.7-m (35.0-ft) screen height.

[3] This restriction is only applied if variable-length landing gear is not assumed to be available.

nominal-mission block fuel burn. For the HWB aircraft, the contrasting results obtained with and without imposing the rotation constraint show that this design requirement has a significant impact on block fuel burn performance.

5.1 Conventional Tube-and-Wing Aircraft

The optimized CTW100 resulting from the conceptual-design phase is shown in Figure 2, and a summary of its characteristics is provided in Table 4. Figure 3 shows the overall design features and flow characteristics for the CTW100 aircraft resulting from the subsequent application of high-fidelity aerodynamic shape optimization. From the top left of Figure 3, it is apparent that the optimizer is successful in essentially eliminating the shocks present over the initial high-fidelity geometry, which was constructed with the RAE-2822 supercritical airfoil. The pressure distributions shown in the right of 3 corroborate this observation, as the sharp increases in pressure present over the initial wing are replaced by smooth pressure recoveries over the optimized wing. The optimized wing features washout toward the tip, which helps achieve an efficient lift distribution, and the isobars are well aligned over its upper surface, which is consistent with low-wave-drag designs.

Grid-converged aerodynamic functionals are estimated by applying Richardson extrapolation to a grid-convergence study conducted on the optimized geometry. The cruise lift-to-drag ratio obtained for the optimized wing-body-tail model is 22.3. Introducing low-fidelity estimates of the contributions not included in the high-fidelity analysis, *i.e.* the excrescence drag and the drag from the vertical tail, nacelles, and pylons, the cruise lift-to-drag ratio becomes 19.0. The block fuel burn over the nominal mission can then be obtained by adding the contributions from all mission segments, giving a value of 2 280 kg (5 027 lb).

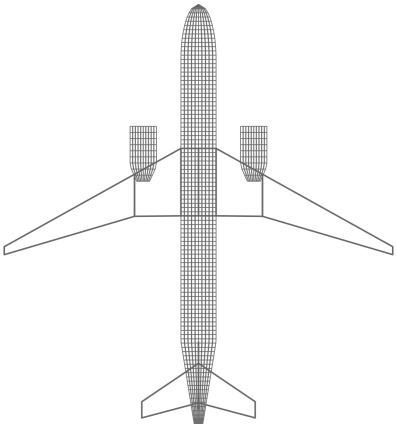

Figure 2 – Conceptual design of the CTW100.

Table 4 – CTW100: Conceptual design results and final block fuel burn estimate. Cruise data are reported at the start of cruise for the nominal mission.

Reference MAC [m]	3.908
Reference area [m^2]	104.9
Wing span [m]	33.71
Wing aspect ratio	10.84
MTOW [kg]	56 400
MZFW [kg]	46 700
OEW [kg]	33 000
MFW [kg]	13 700
Maximum takeoff thrust (per engine) [kN]	92.8
Cruise TSFC [g/s/kN]	16.6
Mach number	0.78
Altitude [m]	11 280
Cruise Reynolds number [$\times$ 10^6]	22.0
Cruise L/D	18.1
Cruise C_L	0.468
Cruise C_D	0.0259
Cruise drag [kN]	25.0
Block fuel burn (Phase One estimate) [kg]	2 340
Block fuel burn (Phase Two estimate) [kg]	2 280

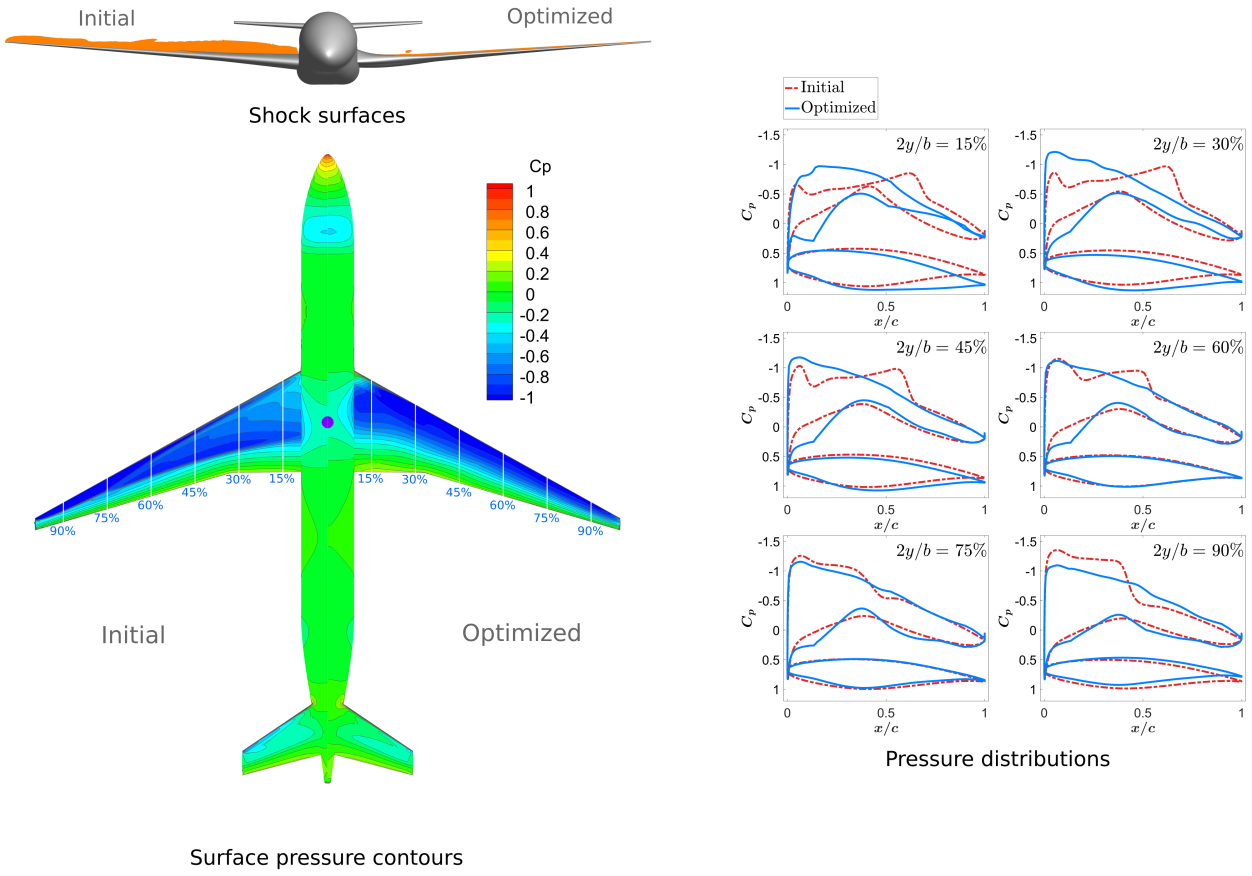

Figure 3 – CTW100: Initial and optimized design and flow features. Flow features are computed on the optimization-level grid at C_L = 0.468.

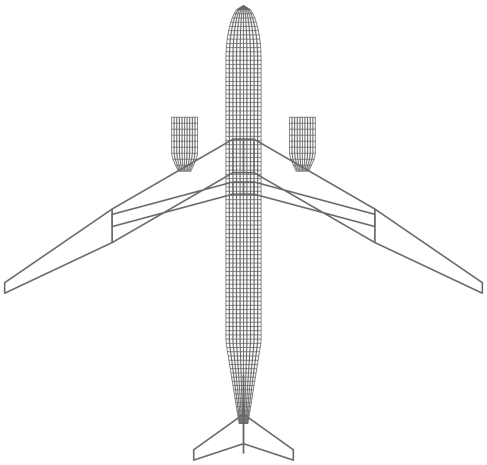

Figure 4 – Conceptual design of the SBW100.

Table 5 – SBW100: Conceptual design results and final block fuel burn estimate. Cruise data are reported at the start of cruise for the nominal mission.

Reference MAC [m]	2.545
Reference area [m^2]	99.22
Wing span [m]	41.45
Wing aspect ratio	17.32
MTOW [kg]	53 400
MZFW [kg]	44 800
OEW [kg]	31 100
MFW [kg]	11 900
Maximum takeoff thrust (per engine) [kN]	88.0
Cruise TSFC [g/s/kN]	16.7
Mach number	0.78
Altitude [m]	13 620
Reynolds number [$\times 10^6$]	9.92
Cruise L/D	21.0
Cruise C_L	0.682
Cruise C_D	0.0324
Cruise drag [kN]	20.5
Block fuel burn (Phase One estimate) [kg]	2 140
Block fuel burn (Phase Two estimate) [kg]	2 110

5.2 Strut-Braced-Wing Aircraft

The optimized SBW100 aircraft resulting from the conceptual-design phase is shown in Figure 4, and a summary of its characteristics is provided in Table 5. The wing span is held fixed based on the Boeing SUGAR High, and its area is sized through chord-length variations by the constraint on the maximum design wing loading, giving it an aspect ratio of 17.32. Compared to the CTW100, the design weights of the SBW100 are generally lower. The wing of the SBW100 weighs 24.5% less than that of the CTW100, demonstrating the structural efficiency provided by the strut, as well as the benefit of a composite construction. The weight of the T-tail is also less than that of the conventional tail of the CTW100, owing primarily to an increased tail moment arm, which allows for a downsizing of the planform area. This causes an increase in the weight of the fuselage, however, due to the increased fuselage bending loads. The engines are sized by the top-of-climb excess-thrust requirement for the nominal mission, which is optimally flown at a higher altitude than the sizing missions for which weight is significantly higher. Since the propulsion system is primarily sized by the minimum thrust-to-weight ratio constraint, the maximum thrust scales with the relative MTOW, which is 5.3% less for the SBW100. Although this translates to an overall reduction in the weight and drag of the propulsion system, the conceptual models predict a small penalty in cruise thrust specific fuel consumption (TSFC). This correlates with a reduction in the capture area or bypass ratio of the engines. The conceptual-level models predict a 16.0% improvement in the cruise lift-to-drag ratio and an 18.0% reduction in cruise drag for the nominal mission. This partly comes from a 59.8% higher wing aspect ratio, thinner wings, and an initial cruise altitude increased from 11 280 m (37 000 ft) to 13 620 m (44 670 ft), which is consistent with the fact that the optimal altitude increases with aspect ratio [4]. Finally, the cruise lift coefficient is 0.682, which indicates that zero-lift and lift-dependent drag forces are rebalanced at high altitude through an increase in induced drag.

Figure 5 shows the overall design features and flow characteristics for the optimized SBW100 resulting from high-fidelity aerodynamic shape optimization. From the top left of 5, it can be seen that the optimizer was not only successful in essentially eliminating the shock waves present over the

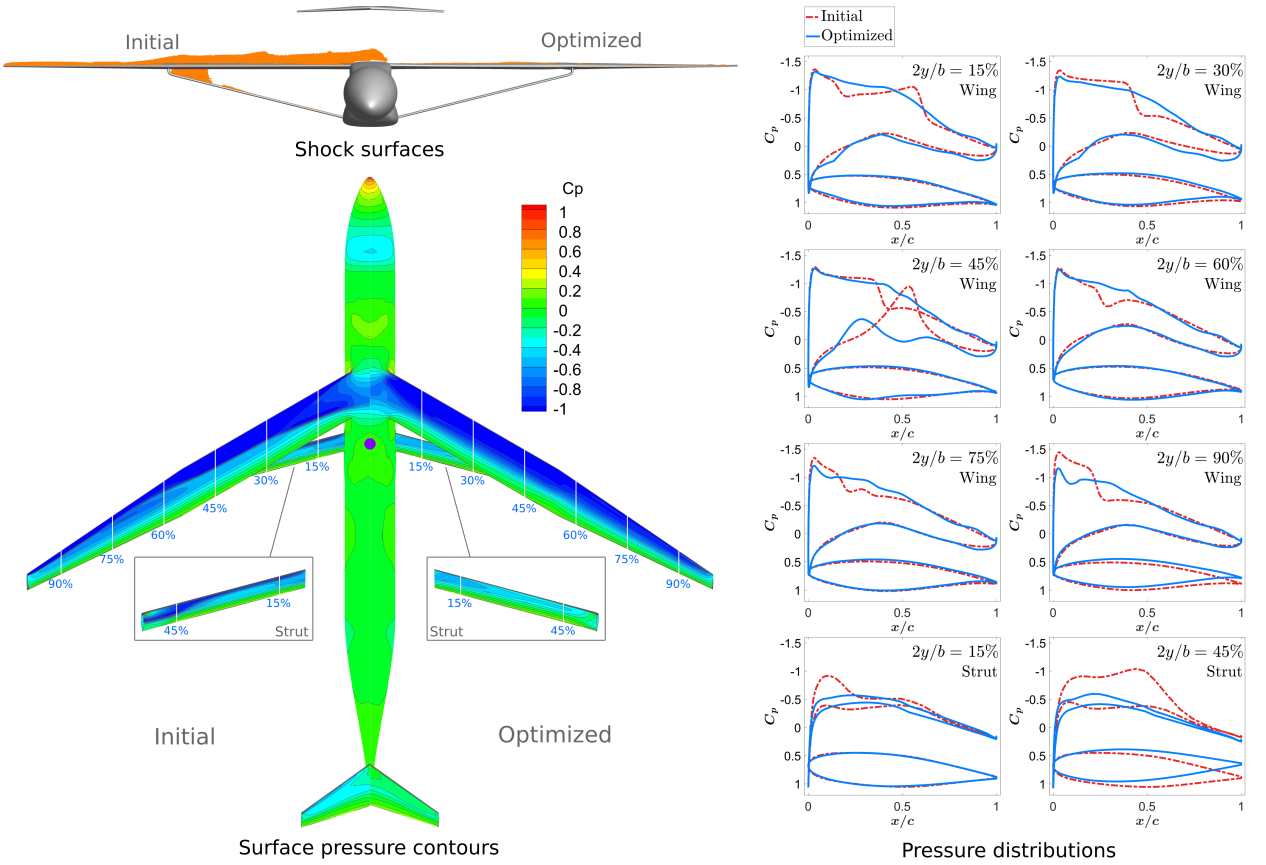

Figure 5 – SBW100: Initial and optimized design and flow features. Flow features are computed on the optimization-level grid at $C_L = 0.682$.

initial wing, but also those near the wing-strut junction. This is consistent with the pressure distributions shown on the right of 5, which indicate that the steep pressure recoveries have been smoothed out. The wing section at 45% semispan also indicates that the shock wave initially present near the wing-strut junction is caused by a rapid acceleration of the flow under the lower surface of the wing, which is likely due to the transonic channel effect. By introducing novel airfoil shapes, the optimizer was successful in mitigating this acceleration and achieving a relatively smooth pressure distribution. Finally, from the bottom left of 5, the surface pressure contours illustrate that the optimizer was again capable of aligning the isobars with the geometric sweep of the wing.

The estimates of the grid-converged aerodynamic functionals obtained through Richardson extrapolation place the cruise lift-to-drag ratio of the wing-body-tail geometry at 24.5. Introducing the low-fidelity estimates of the contributions to drag not included in the high-fidelity analysis, the cruise lift-to-drag ratio becomes 21.4 for the full aircraft. The block fuel burn is then calculated to be 2 110 kg (4 650 lb), which translates to a 7.6% savings over the relatively short nominal mission when compared to the optimized CTW100. Overall, these results demonstrate the ability of high-fidelity aerodynamic shape optimization to address the aerodynamic challenges of designing a transonic SBW aircraft at a relatively high optimal lift coefficient of 0.682.

5.3 Hybrid-Wing-Body Aircraft

The characteristics of the HWB100 aircraft resulting from the application of multifidelity multidisciplinary optimization at 13 410 m (44 000 ft) with and without a rotation constraint are summarized in Table 6, and the optimal geometries are shown in Figure 6. Among the three tested initial cruise altitudes of 10 970 m (36 000 ft), 12 190 m (40 000 ft), and 13 410 m (44 000 ft), the HWB100 is most efficient at the highest altitude. This is again consistent with expectations, as the optimal cruise altitude of an aircraft increases with respect to decreasing wing loading [4]. The aircraft optimized with a rotation constraint burns 2 020 kg of fuel, or 11.5% less than the CTW100, over the nominal mis-

Table 6 – HWB100: Multifidelity multidisciplinary optimization results. Cruise data are reported at the start of cruise for the nominal mission.

Rotation modeled as:	Model 1 [1]	Model 2 [2]
Reference MAC [m]	12.92	12.92
Reference area [m^2]	276.6	252.8
Wing span [m]	43.08	39.34
Overall aspect ratio	6.709	6.122
MTOW [kg]	51 900	49 100
MZFW [kg]	41 300	39 300
OEW [kg]	30 900	29 000
MFW [kg]	10 600	9 810
Maximum takeoff thrust (per engine) [kN]	99.7	76.8
Cruise TSFC [g/s/kN]	16.6	16.8
Mach number	0.78	0.78
Altitude [m]	13 410	13 410
Reynolds number [$\times$ 10^6]	52.27	52.27
Cruise L/D	22.1	22.4
Cruise C_L	0.231	0.243
Cruise C_D	0.0106	0.0108
Cruise drag [kN]	19.5	18.2
Block fuel burn [kg]	2 020	1 910

[1]Model 1: Initial pitch acceleration of 3 deg/s^2 at rotation.

[2]Model 2: Assumes that variable-length landing gear technology is used [62, 63].

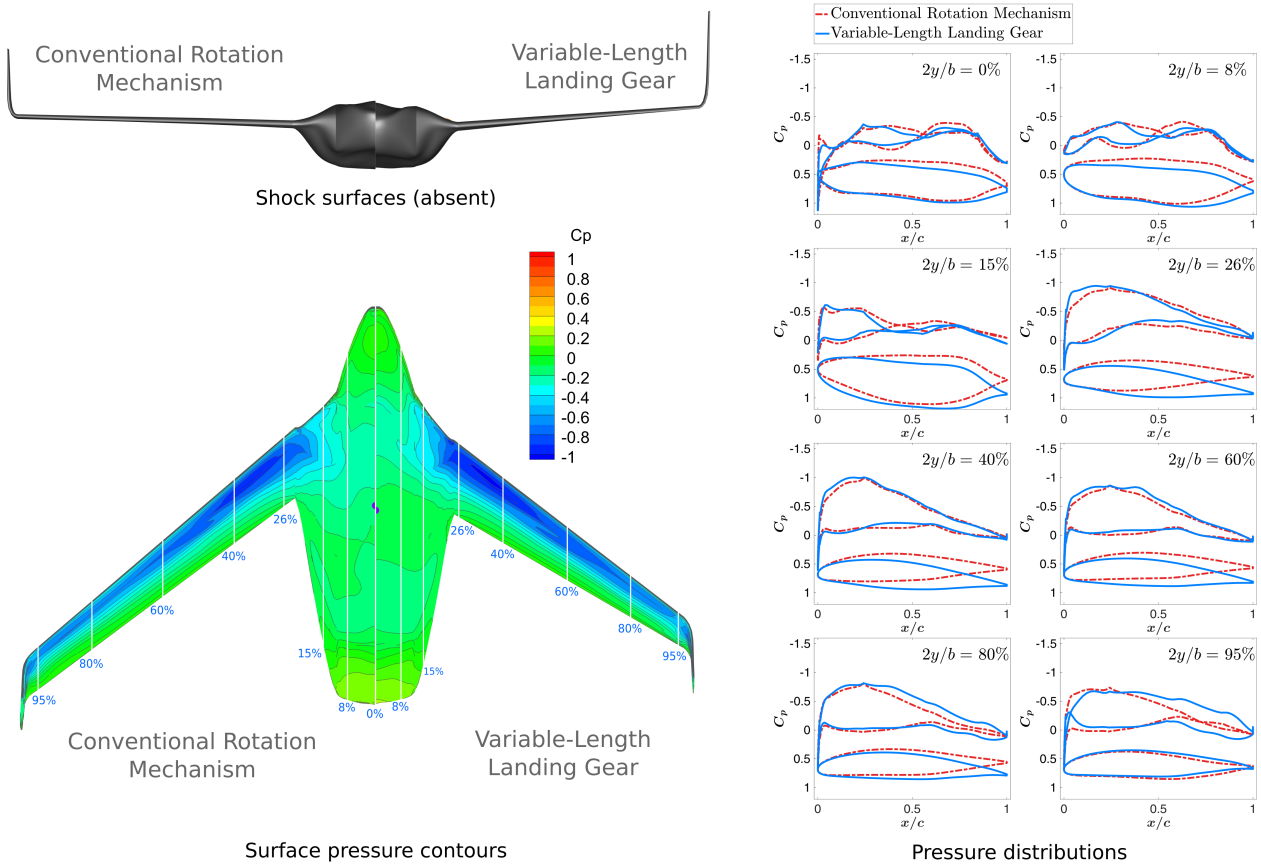

Figure 6 – HWB100: Optimized designs with and without imposing a rotation constraint. Flow features are computed on the optimization-level grid at C_L = 0.231 (left) and C_L = 0.243 (right).

sion, while the aircraft optimized without the rotation constraint burns 1 910 kg of fuel, or 16.3% less than the CTW100. As for the CTW100 and SBW100, both figures are calculated through Richardson extrapolation on the optimized geometry and include the low-fidelity estimates of the contributions to drag not included in the high-fidelity aerodynamic analysis. All the constraints discussed in Section 4.3 are active except that on wingtip ground-strikes, indicating that they have some effect on block fuel burn. Comparing both versions of the HWB100 aircraft shown in Figure 6, it can be seen that the planforms are significantly different, and so are many airfoil profiles. The observations and data above lead directly to two conclusions: 1) if variable-length landing gear is not assumed to be available, then imposing the design requirement captured by the rotation constraint is essential in estimating the block-fuel-burn benefit of the HWB100, and 2) the HWB100 is significantly penalized by such a design requirement, the block-fuel-burn penalty being 5.7%. Nonetheless, a substantial benefit was achieved with respect to the CTW100 in either case by making liberal use of the available geometric freedom. The discussion below is centered on arguing the necessity of using a coupled multifidelity multidisciplinary optimization framework with ample geometric freedom, which can optimally satisfy the design requirements by designing complex multifunctional aerodynamic surfaces.

The role of sectional geometric freedom in the automatic generation of two nonstandard design features is discussed first. As seen on the 8%- and 15%-span pressure distributions in Figure 6, the transition region (between the centerbody and wing) and a certain portion of the centerbody has been distinctly frontloaded, namely through twist or by manipulating the section-shape design variables. On the 15%-span cross-section of the geometry optimized without assuming variable-length landing gear, the optimizer created a slight indent on the underside near the leading edge, consistent with a previously reported mechanism to help alleviate trim drag at cruise through frontloading these long cross-sections [64]. This frontloading also helps produce a nose-up pitching moment to assist with rotation after the pitch effectors are fully relied upon. Nearby, on the centerbody, the section shapes feature a distinct bump on their upper surface, which forms a ridge. This is best seen on the forward-facing geometry shown on the upper left of Figure 6. The optimizer has created this design feature to help with efficiently lifting the MTOW at low-speed by making use of vortex lift over the centerbody instead of further increasing the planform area. The design features discussed above significantly improve performance compared to cases where nonlinear spanwise variations in twist angles and section shapes were not allowed [19].

The role of planform geometric freedom in satisfying the rotation constraint is discussed next. In the case without the rotation constraint, the position of the wingtip is largely driven by the OEI directional-trim constraint, as the rudders are attached to the large winglets. The need to reduce or eliminate shocks at cruise through wing sweep also contributes to the position of the wingtip, but wing sweep can be partly designed through moving the wing root fore or aft. Needing to satisfy the rotation constraint has rendered optimal an increase in wing sweep, wing span, and wingtip chord lengths beyond what was otherwise necessary, as each increases the effectiveness of the pitch effectors, and it has resulted in the wing roots being moved relatively far forward. The chord and span of the centerbody elevator were not significantly increased, despite its long lever arm, because this would imply increasing the dimensions of the centerbody, whose weight increases at a faster rate with respect to span than that of the wing, and because its CG is more forward than that of the wing.

Despite the high initial cruise altitude, the engines are sized by takeoff requirements, and not by their ability to provide a rate of climb of 1.52 m/s (300 ft/min) at the top of climb. Removing the rotation constraint has a substantial impact on engine size: 23.0% less sea-level-static thrust is needed to satisfy the takeoff-field-length constraint in that case. This is partly because a lower rotation speed is needed without the rotation constraint, and a lighter aircraft with decreased pitch-effector surface area is designed.

6 Conclusions

As a result of their potential for improved energy efficiency relative to the established CTW aircraft configuration, unconventional aircraft configurations are likely to play an important role in reducing the

impact of civil aviation on climate change. It is therefore important to address the major design challenges associated with specific unconventional configurations and to aim to obtain credible estimates of their energy-efficiency benefits relative to the CTW configuration. Although low- to medium-fidelity conceptual-level tools can provide reasonable accuracy for the CTW configuration, their credibility for unconventional configurations is more limited. These aircraft configurations benefit from optimization based on high-fidelity aerodynamics models both to address key complex aerodynamic design challenges and to obtain accurate estimates of their energy efficiency.

In this paper, guiding principles for the formulation of cost-efficient and accurate multifidelity multidisciplinary optimization problems have been presented. Four main considerations were discussed, namely 1) the selection of the design requirements, enforced as constraints in an optimization problem, that are most critical to the accurate computation of the performance metric, and the determination of the aircraft-design disciplines that chiefly determine whether these design requirements are satisfied; 2) the selection of physical-model fidelity levels that best balance computational cost and accuracy; 3) the selection of design variables and constraints that allow an optimizer to realize the potential of a given unconventional aircraft configuration without introducing unnecessary manufacturing difficulties or inhibiting the convergence of the optimization problem; and 4) the structuring of the optimization process in terms of whether each design variable should be optimized simultaneously or whether the aircraft configuration and the selected design variables are amenable to a decoupled approach to optimization.

Specialized optimization tools were then described, ranging from conceptual-level tools to a high-fidelity aerodynamic shape optimization framework that allows considerable geometric freedom and is flexible to the inclusion of non-aerodynamics disciplines. Then, the guiding principles were applied to formulate optimization problems for comparative studies of regional-class SBW and HWB aircraft relative to a reference CTW aircraft. Block fuel burn was selected as the performance metric, current technology levels were considered, the Embraer E190-E2 was selected as a reference aircraft, and representative nominal and sizing missions were specified. The regional-class SBW aircraft provides a 7.6% block-fuel-burn benefit over the 500-nmi nominal mission, while the regional-class HWB aircraft provides an 11.5% benefit if rotation is required to be achieved through conventional means, and a 16.3% benefit when assuming that variable-length landing gear actuated by downforce is available.

A further increase in credibility can be obtained by testing some of the assumptions made in this work, namely whether the relative block fuel burn of each unconventional aircraft is indeed negligibly sensitive to buffet and flutter considerations. This will require the integration of efficient buffet [65] and flutter constraints [66, 67] into the optimization framework. Finally, optimizing performance over a range of cruise operating conditions can help ensure the robustness of the optimal designs, thus ensuring that one aircraft configuration does not benefit more from being optimized for a single nominal cruise condition than another [33–36].

References

[1] Greitzer, E.M., Bonnefoy, P.A., Hall, D.K., Hansman, R.J., Hileman, J.I., Liebeck, R.H., Lovegren, J., Mody, P., Pertuze, J.A., Sato, S., Spakovszky, Z.S., Tan, C.S., Hollman, J.S., Duda, J.E., Fitzgerald, N., Houghton, J., Kerrebrock, J.L., Kiwada, G.F., Kordonowy, D., Parrish, J.C., Tylko, J., and Wen, E.A. "N+3 Aircraft Concept Designs and Trade Studies, Final Report". *Tech. Rep. NASA/CR-2010-216794/VOL1*, National Aeronautics and Space Administration, Cleveland, Ohio, USA, 2010.

[2] Gagnon, H. and Zingg, D.W. "Euler-Equation-Based Drag Minimization of Unconventional Aircraft Configurations". *Journal of Aircraft*, vol. 53(5): pp. 1361–1371, 2016. doi:10.2514/1.C033591.

[3] Faggiano, F., Vos, R., Baan, M., and Van Dijk, R. "Aerodynamic Design of a Flying V Aircraft". 17th AIAA Aviation Technology, Integration, and Operations Conference. American Institute of Aeronautics and Astronautics. Paper 2017-3589, Denver, Colorado, USA, 2017. doi:10.2514/6.2017-3589.

[4] Bravo-Mosquera, P.D., Catalano, F.M., and Zingg, D.W. "Unconventional Aircraft for Civil Aviation: A Review of Concepts and Design Methodologies". *Progress in Aerospace Sciences*, vol. 131: pp. 1–29, 2022. doi:10.1016/j.paerosci.2022.100813.

[5] Wick, A.T., Hooker, J.R., and Zeune, C.H. "Integrated Aerodynamic Benefits of Distributed Propulsion".

53rd AIAA Aerospace Sciences Meeting. American Institute of Aeronautics and Astronautics. Paper 2015-1500, Kissimmee, Florida, USA, 2015. doi:10.2514/6.2015-1500.

[6] Harrison, N., Anderson, J., Fleming, J., and Ng, W. "Experimental Investigation of Active Flow Control of a Boundary Layer Ingesting Serpentine Inlet Diffuser". 45th AIAA Aerospace Sciences Meeting and Exhibit. American Institute of Aeronautics and Astronautics. Paper 2007-843, Reno, NV, USA, 2007. doi:10.2514/6.2007-843.

[7] Green, J. "Laminar Flow Control - Back to the Future?" 38th Fluid Dynamics Conference and Exhibit. American Institute of Aeronautics and Astronautics. Paper 2008-3738, Seattle, Washington, 2008. doi:10.2514/6.2008-3738.

[8] Raymer, D.P. *Aircraft Design: a Conceptual Approach*. American Institute of Aeronautics and Astronautics, Reston, Virginia, USA, 6th ed., 2018.

[9] Torenbeek, E. *Synthesis of Subsonic Airplane Design*. Springer Science+Business Media, B.V., Dordrecht, Netherlands, 1st ed., 1982.

[10] Hicken, J.E. and Zingg, D.W. "Aerodynamic Optimization Algorithm with Integrated Geometry Parameterization and Mesh Movement". *AIAA Journal*, vol. 48(2): pp. 400–413, 2010. doi:10.2514/1.44033.

[11] Carrier, G., Destarac, D., Dumont, A., Meheut, M., Salah El Din, I., Peter, J., Ben Khelil, S., Brezillon, J., and Pestana, M. "Gradient-Based Aerodynamic Optimization with the elsA Software". 52nd AIAA Aerospace Sciences Meeting. American Institute of Aeronautics and Astronautics. Paper 2014-0568, National Harbor, Maryland, USA, 2014. doi:10.2514/6.2014-0568.

[12] Osusky, L., Buckley, H., Reist, T., and Zingg, D.W. "Drag Minimization Based on the Navier–Stokes Equations Using a Newton–Krylov Approach". *AIAA Journal*, vol. 53(6): pp. 1555–1577, 2015. doi:10.2514/1.J053457.

[13] Riggins, B., Locatelli, D., Schetz, J., Kapania, R., and Poquet, T. "Development of a Multi-Disciplinary Optimization Framework for Nonconventional Aircraft Configurations in PACELAB APD". p. 21. SAE 2015 AeroTech Congress & Exhibition. SAE International. Paper 2015-01-2564, 2015. doi:10.4271/2015-01-2564.

[14] Economon, T.D., Palacios, F., Copeland, S.R., Lukaczyk, T.W., and Alonso, J.J. "SU2: An Open-Source Suite for Multiphysics Simulation and Design". *AIAA Journal*, vol. 54(3): pp. 828–846, 2016. doi:10.2514/1.J053813.

[15] MacDonald, T., Clarke, M., Botero, E.M., Vegh, J.M., and Alonso, J.J. "SUAVE: An Open-Source Environment Enabling Multi-Fidelity Vehicle Optimization". 18th AIAA/ISSMO Multidisciplinary Analysis and Optimization Conference. American Institute of Aeronautics and Astronautics. Paper 2017-4437, Denver, Colorado, USA, 2017. doi:10.2514/6.2017-4437.

[16] Gray, J.S., Hwang, J.T., Martins, J.R.R.A., Moore, K.T., and Naylor, B.A. "OpenMDAO: an Open-source Framework for Multidisciplinary Design, Analysis, and Optimization". *Structural and Multidisciplinary Optimization*, vol. 59(4): pp. 1075–1104, 2019. doi:10.1007/s00158-019-02211-z.

[17] Reist, T.A., Zingg, D.W., Rakowitz, M., Potter, G., and Banerjee, S. "Multifidelity Optimization of Hybrid Wing–Body Aircraft with Stability and Control Requirements". *Journal of Aircraft*, vol. 56(2): pp. 442–456, 2019. doi:10.2514/1.C034703.

[18] Feldstein, A., Lazzara, D., Princen, N., and Willcox, K. "Multifidelity Data Fusion: Application to Blended-Wing-Body Multidisciplinary Analysis Under Uncertainty". *AIAA Journal*, vol. 58(2): pp. 889–906, 2020. doi:10.2514/1.J058388.

[19] Gray, A.L., Reist, T.A., and Zingg, D.W. "Further Exploration of Regional-Class Hybrid Wing-Body Aircraft Through Multifidelity Optimization". AIAA SciTech 2021 Forum. American Institute of Aeronautics and Astronautics. Paper 2021-0014, Virtual event, 2021. doi:10.2514/6.2021-0014.

[20] Kafkas, A., Kilimtzidis, S., Kotzakolios, A., Kostopoulos, V., and Lampeas, G. "Multi-Fidelity Optimization of a Composite Airliner Wing Subject to Structural and Aeroelastic Constraints". *Aerospace*, vol. 8(12): p. 398, 2021. doi:10.3390/aerospace8120398.

[21] Chau, T. and Zingg, D.W. "Aerodynamic Design Optimization of a Transonic Strut-Braced-Wing Regional Aircraft". *Journal of Aircraft*, vol. 59(1): pp. 253–271, 2022. doi:10.2514/1.C036389.

[22] Lobo do Vale, J., Sohst, M., Crawford, C., Suleman, A., Potter, G., and Banerjee, S. "On the Multi-Fidelity Approach in Surrogate-Based Multidisciplinary Design Optimisation of High-Aspect-Ratio Wing Aircraft". *The Aeronautical Journal*, pp. 1–22, 2022. doi:10.1017/aer.2022.49.

[23] Peherstorfer, B., Willcox, K., and Gunzburger, M. "Survey of Multifidelity Methods in Uncertainty Propagation, Inference, and Optimization". *SIAM Review*, vol. 60(3): pp. 550–591, 2018. doi:10.1137/16M1082469.

[24] Leung, T.M. and Zingg, D.W. "Aerodynamic Shape Optimization of Wings Using a Parallel Newton-Krylov

Approach". *AIAA Journal*, vol. 50(3): pp. 540–550, 2012. doi:10.2514/1.J051192.

[25] Kenway, G.K.W., Kennedy, G.J., and Martins, J.R.R.A. "Scalable Parallel Approach for High-Fidelity Steady-State Aeroelastic Analysis and Adjoint Derivative Computations". *AIAA Journal*, vol. 52(5): pp. 935–951, 2014. doi:10.2514/1.J052255.

[26] Zhang, Z.J., Khosravi, S., and Zingg, D.W. "High-Fidelity Aerostructural Optimization with Integrated Geometry Parameterization and Mesh Movement". *Structural and Multidisciplinary Optimization*, vol. 55(4): pp. 1217–1235, 2017. doi:10.1007/s00158-016-1562-7.

[27] Gray, J.S., Mader, C.A., Kenway, G.K.W., and Martins, J.R.R.A. "Modeling Boundary Layer Ingestion Using a Coupled Aeropropulsive Analysis". *Journal of Aircraft*, vol. 55(3): pp. 1191–1199, 2018. doi:10.2514/1.C034601.

[28] Yildirim, A., Gray, J.S., Mader, C.A., and Martins, J.R.R.A. "Aeropropulsive Design Optimization of a Boundary Layer Ingestion System". AIAA Aviation 2019 Forum. American Institute of Aeronautics and Astronautics. Paper 2019-3455, Dallas, Texas, USA, 2019. doi:10.2514/6.2019-3455.

[29] Gagnon, H. and Zingg, D.W. "Two-Level Free-Form and Axial Deformation for Exploratory Aerodynamic Shape Optimization". *AIAA Journal*, vol. 53(7): pp. 2015–2026, 2015. doi:10.2514/1.J053575.

[30] Viti, A., Druot, T., and Dumont, A. "Aero-Structural Approach Coupled with Direct Operative Cost Optimization for New Aircraft Concept in Preliminary Design". 17th AIAA/ISSMO Multidisciplinary Analysis and Optimization Conference. American Institute of Aeronautics and Astronautics. Paper 2016-3512, Washington, D.C., USA, 2016. doi:10.2514/6.2016-3512.

[31] Green, J.E. "Civil Aviation and the Environment – the Next Frontier for the Aerodynamicist". *The Aeronautical Journal*, vol. 110(1110): pp. 469–486, 2006. doi:10.1017/S0001924000001378.

[32] Proesmans, P.J. and Vos, R. "Airplane Design Optimization for Minimal Global Warming Impact". AIAA Scitech 2021 Forum. American Institute of Aeronautics and Astronautics. Paper 2021-1297, Virtual event, 2021. doi:10.2514/6.2021-1297.

[33] Nemec, M., Zingg, D.W., and Pulliam, T.H. "Multipoint and Multi-Objective Aerodynamic Shape Optimization". *AIAA Journal*, vol. 42(6): pp. 1057–1065, 2004. doi:10.2514/1.10415.

[34] Kenway, G.K.W. and Martins, J.R.R.A. "Multipoint High-Fidelity Aerostructural Optimization of a Transport Aircraft Configuration". *Journal of Aircraft*, vol. 51(1): pp. 144–160, 2014. doi:10.2514/1.C032150.

[35] Bons, N., Mader, C.A., Martins, J.R.R.A., Cuco, A., and Odaguil, F. "High-Fidelity Aerodynamic Shape Optimization of a Full Configuration Regional Jet". AIAA Scitech 2022 Forum. American Institute of Aeronautics and Astronautics. Paper 2018-0106, Kissimmee, Florida, USA, 2018. doi:10.2514/6.2018-0106.

[36] Chau, T. and Zingg, D.W. "Fuel Burn Evaluation of a Transonic Strut-Braced-Wing Regional Aircraft Through Multipoint Aerodynamic Optimisation". *The Aeronautical Journal*, pp. 1–25, 2022. doi:10.1017/aer.2022.64.

[37] Bower, G. and Kroo, I. "Multi-Objective Aircraft Optimization for Minimum Cost and Emissions over Specific Route Networks". The 26th Congress of ICAS and 8th AIAA ATIO. American Institute of Aeronautics and Astronautics. Paper 2008-8905, Anchorage, Alaska, USA, 2008. doi:10.2514/6.2008-8905.

[38] Chiang, C., Koo, D., and Zingg, D.W. "Aerodynamic Shape Optimization of an S-Duct Intake for a Boundary-Layer Ingesting Engine". *Journal of Aircraft*, vol. 59(3): pp. 725–741, 2022. doi:10.2514/1.C036632.

[39] Streuber, G.M. and Zingg, D.W. "Evaluating the Risk of Local Optima in Aerodynamic Shape Optimization". *AIAA Journal*, vol. 59(1): pp. 75–87, 2021. doi:10.2514/1.J059826.

[40] Streuber, G.M. and Zingg, D.W. "Dynamic Geometry Control for Robust Aerodynamic Shape Optimization". AIAA Aviation 2021 Forum. American Institute of Aeronautics and Astronautics. Paper 2021-3031, Virtual Event, 2021. doi:10.2514/6.2021-3031.

[41] Malone, B. and Mason, W.H. "Multidisciplinary Optimization in Aircraft Design Using Analytic Technology Models". AIAA/AHS/ASEE Aircraft Design Systems and Opterations Meeting. American Institute of Aeronautics and Astronautics. Paper 91-3187, Baltimore, Maryland, USA, 1991. doi:10.2514/6.1991-3187.

[42] Kroo, I. and Shevell, R. "Aircraft Design, Synthesis and Analysis". *Document [retrieved 23 dec. 2016]*, Stanford University. URL `https://adg.stanford.edu/aa241/AircraftDesign.html`.

[43] Andrews, S.A., Perez, R.E., and Wowk, D. "Wing Weight Model for Conceptual Design of Nonplanar Configurations". *Aerospace Science and Technology*, vol. 43(1): pp. 51–62, 2015. doi:10.1016/j.ast.2015.02.011.

[44] Torenbeek, E. "Development and Application of a Comprehensive, Design-Sensitive Weight Prediction Method for Wing Structures of Transport Category Aircraft". *Tech. Rep. LR-693*, Delft University of Technology, Dordrecht, Netherlands, 1992.

[45] Gur, O., Bhatia, M., Mason, W., Schetz, J., Kapania, R., and Nam, T. "Development of Framework for

Truss-Braced Wing Conceptual MDO". 51st AIAA/ASME/ASCE/AHS/ASC Structures, Structural Dynamics, and Materials Conference. American Institute of Aeronautics and Astronautics. Paper 2010-2754, Orlando, Florida, USA, 2010. doi:10.2514/6.2010-2754.

[46] "The USAF Stability and Control Digital DATCOM. Volume II. Implementation of Datcom Methods." *Tech. Rep. ADA086558*, McDonnell Douglas Astronautics Co., St. Louis, Missouri, USA, 1979.

[47] Telidetzki, K., Osusky, L., and Zingg, D.W. "Application of Jetstream to a Suite of Aerodynamic Shape Optimization Problems". 52nd Aerospace Sciences Meeting. American Institute of Aeronautics and Astronautics. Paper 2014-0571, National Harbor, Maryland, USA, 2014. doi:10.2514/6.2014-0571.

[48] Lee, C., Koo, D., Telidetzki, K., Buckley, H., Gagnon, H., and Zingg, D.W. "Aerodynamic Shape Optimization of Benchmark Problems Using Jetstream". 53rd AIAA Aerospace Sciences Meeting. American Institute of Aeronautics and Astronautics. Paper 2015-0262, Kissimmee, Florida, USA, 2015. doi:10.2514/6.2015-0262.

[49] Reist, T.A., Koo, D., Zingg, D.W., Bochud, P., Castonguay, P., and Leblond, D. "Cross Validation of Aerodynamic Shape Optimization Methodologies for Aircraft Wing-Body Optimization". *AIAA Journal*, vol. 58(6): pp. 2581–2595, 2020. doi:10.2514/1.J059091.

[50] Osusky, M., Boom, P.D., and Zingg, D.W. "Results from the Fifth AIAA Drag Prediction Workshop Obtained with a Parallel Newton-Krylov-Schur Flow Solver Discretized Using Summation-by-Parts Operators". 31st AIAA Applied Aerodynamics Conference. American Institute of Aeronautics and Astronautics. Paper 2013-2511, San Diego, California, USA, 2013. doi:10.2514/6.2013-2511.

[51] Gill, P.E., Murray, W., and Saunders, M.A. "SNOPT: An SQP Algorithm for Large-Scale Constrained Optimization". *SIAM Journal of Optimization*, vol. 12(4): pp. 979–1006, 2002. doi:10.1137/S0036144504446096.

[52] Hicken, J.E. and Zingg, D.W. "A Simplified and Flexible Variant of GCROT for Solving Nonsymmetric Linear Systems". *SIAM Journal on Scientific Computing*, vol. 32(3): pp. 1672–1694, 2010. doi:10.1137/090754674.

[53] Bradley, K.R. "A Sizing Methodology for the Conceptual Design of Blended-Wing-Body Transports". *Tech. Rep. NASA/CR-2004-213016*, NASA Langley Research Center: Joint Institute for Advancement of Flight Sciences, Hampton, Virginia, USA, 2004.

[54] "E-Jets E2 Airport Planning Manual". *Tech. Rep. APM - 5824*, Embraer S.A., Sao Jose Dos Campos, Brazil, 2019.

[55] "Type-Certificate Data Sheet - Pratt & Whitney PW1500G Series Engines". *Tech. Rep. No. : IM.E.090*, European Union Aviation Safety Agency, 2021.

[56] Pfenninger, W. "Design Considerations of Large Subsonic Long Range Transport Airplanes with Low Drag Boundary Layer Suction". *Tech. Rep. NAI-54-800 (BLC-67)*, Northrop Aircraft Incorporated, 1954.

[57] Meadows, N.A., Schetz, J.A., Kapania, R.K., Bhatia, M., and Seber, G. "Multidisciplinary Design Optimization of Medium-Range Transonic Truss-Braced Wing Transport Aircraft". *Journal of Aircraft*, vol. 49(6): pp. 1006–1014, 2012. doi:10.2514/1.C031695.

[58] Chakraborty, I., Nam, T., Gross, J.R., Mavris, D.N., Schetz, J.A., and Kapania, R.K. "Comparative Assessment of Strut-Braced and Truss-Braced Wing Configurations Using Multidisciplinary Design Optimization". *Journal of Aircraft*, vol. 52(6): pp. 2009–2020, 2015. doi:10.2514/1.C033120.

[59] Carrier, G.G., Arnoult, G., Fabbiane, N., Schotte, J.S., David, C., Defoort, S., Benard, E., and Delavenne, M. "Multidisciplinary Analysis and Design of Strut-Braced Wing Concept for Medium Range Aircraft". AIAA Scitech 2022 Forum. American Institute of Aeronautics and Astronautics. Paper 2022-0726, San Diego, California, USA & Virtual event, 2022. doi:10.2514/6.2022-0726.

[60] Bradley, M.K., Droney, C., and Allen, T.J. "Subsonic Ultra Green Aircraft Research". *Tech. Rep. NASA/CR-2015-218704/Volume I*, Boeing Research and Technology, Huntington Beach, California, USA, 2015.

[61] Liebeck, R.H. "Design of the Blended Wing Body Subsonic Transport". *Journal of Aircraft*, vol. 41(1): pp. 10–25, 2004. doi:10.2514/1.9084.

[62] Page, M.A. "Tilting Landing Gear Systems and Methods". *Patent US 2018/0001999 A1*, Tucson, Arizona, USA, 2018.

[63] Yang, S., Page, M., and Smetak, E.J. "Achievement of NASA New Aviation Horizons N+2 Goals with a Blended-Wing-Body X-Plane Designed for the Regional Jet and Single-Aisle Jet Markets". 2018 AIAA Aerospace Sciences Meeting. American Institute of Aeronautics and Astronautics. Paper 2018-0521, Kissimmee, Florida, USA, 2018. doi:10.2514/6.2018-0521.

[64] Sargeant, M.A., Hynes, T.P., Graham, W.R., Hileman, J.I., Drela, M., and Spakovszky, Z.S. "Stability of Hybrid-Wing-Body-Type Aircraft with Centerbody Leading-Edge Carving". *Journal of Aircraft*, vol. 47(3): pp. 970–974, 2010. doi:10.2514/1.46544.

[65] Kenway, G.K.W. and Martins, J.R.R.A. "Buffet-Onset Constraint Formulation for Aerodynamic Shape Optimization". *AIAA Journal*, vol. 55(6): pp. 1930–1947, 2017. doi:10.2514/1.J055172.

[66] Marques, A.N., Opgenoord, M.M.J., Lam, R.R., Chaudhuri, A., and Willcox, K.E. "Multifidelity Method for Locating Aeroelastic Flutter Boundaries". *AIAA Journal*, vol. 58(4): pp. 1772–1784, 2020. doi:10.2514/1.J058663.

[67] Lowe, B.M. and Zingg, D.W. "Flutter Prediction Using Reduced-Order Modeling with Error Estimation". *AIAA Journal*, pp. 1–16, 2022. doi:10.2514/1.J061389.

Contact Author Email Address

The contact author email address is: dwz@utias.utoronto.ca

Copyright Statement